$H \to \tau^+\tau^-$ branching ratio study at $\sqrt{s} = 250$ GeV at the ILC with the ILD detector

Shin-ichi Kawada[1,†], Keisuke Fujii[2], Taikan Suehara[3], Tohru Takahashi[1], Tomohiko Tanabe[3]

February 2, 2013 (revised at March 22, 2013)

1: Advanced Sciences of Matter (AdSM), Hiroshima University, 1-3-1, Kagamiyama, Higashi-Hiroshima, Hiroshima, 739-8530, Japan
2: High Energy Accelerator Research Organization (KEK), 1-1, Oho, Tsukuba, Ibaraki, 305-0801, Japan
3: International Center for Elementary Particle Physics (ICEPP), The University of Tokyo, 7-3-1, Hongo, Bunkyo-ku, Tokyo, 113-0033, Japan

† : `s-kawada@huhep.org`

Abstract

We evaluated the measurement accuracy of the branching ratio of $H \to \tau^+\tau^-$ mode at $\sqrt{s} = 250$ GeV at the ILC with the ILD detector. We assumed the Higgs mass $M_H = 120$ GeV, branching ratio $\mathrm{Br}(H \to \tau^+\tau^-) = 8.0$ %, beam polarization $P(e^-, e^+) = (-0.8, +0.3)$, and integrated luminosity $\int L\ dt = 250$ fb^{-1}. We used the LOI samples as the Monte-Carlo samples. The evaluation was performed by the ILD full detector simulation. All Standard Model backgrounds were included in this study. We obtained the accuracy $\Delta(\sigma\cdot\mathrm{Br})/(\sigma\cdot\mathrm{Br}) = 3.5$ %. The scaled result to $M_H = 125$ GeV is calculated to be 4.2 %.

1 Introduction

A new Higgs-like particle was discovered by the ATLAS and the CMS experiments [1, 2]. One of the next important themes for particle physics is the investigation of that new particle, especially the mass generation mechanism.

One of the important properties of Higgs boson is its branching ratio. In the Standard Model (SM) of particle physics, the Yukawa coupling constant of matter fermions with the Higgs boson is proportional to the fermion mass. Besides, if there is new physics, the coupling constant may deviate from the SM prediction. Therefore, the branching ratio is a probe for new physics.

In this note, we focus on the branching ratio of $H \to \tau^+\tau^-$ mode. We estimate the measurement accuracy of the $H \to \tau^+\tau^-$ branching ratio at $\sqrt{s} = 250$ GeV with the ILD full detector simulation.

2 Signal and Background

The main Higgs production process at $\sqrt{s} = 250$ GeV is the Higgs-strahlung process ($e^+e^- \to ZH$). There are three types of signal depending on the decay of the Z boson, as shown in Figure 1. In this note, we concentrate on (A) $Z \to l^+l^-$ mode and (B) $Z \to q\bar{q}$ mode.

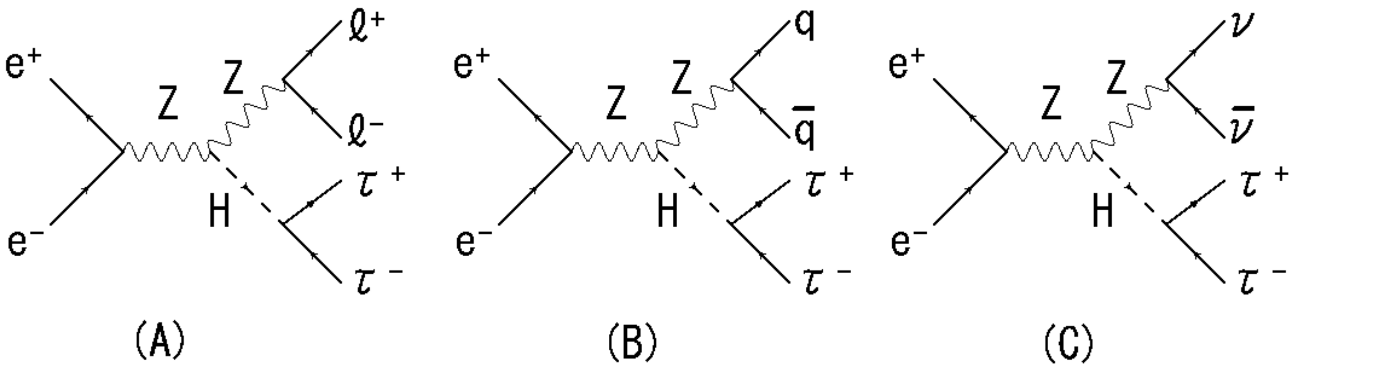

Figure 1: The diagrams of signal processes. (A): $Z \to l^+l^-$ mode, (B): $Z \to q\bar{q}$ mode, (C): $Z \to \nu\bar{\nu}$ mode.

The $Z \to \nu\bar{\nu}$ mode has been found to contribute negligibly to the overall precision which is dominated by the $Z \to q\bar{q}$ mode. However, at higher center-of-mass energies, the $e^+e^- \to \nu\bar{\nu}H$ mode is expected to contribute substantially due to the increase in the cross section of WW fusion process.

2.1 $Z \to l^+l^-$ mode

In this mode, we only considered $Z \to e^+e^-$ mode and $Z \to \mu^+\mu^-$ mode as the signal process. The signal cross section of this mode is 1.9 fb. The dominant background processes are the four leptons processes ($e^+e^- \to eeee$, $ee\mu\mu$, $ee\tau\tau$, $\mu\mu\mu\mu$, $\mu\mu\tau\tau$, and $\tau\tau\tau\tau$). An example diagram is shown in Figure 2-(A). Other background processes are $e^+e^- \to ZH$ reactions where the Higgs boson does not decay to tau pairs.

2.2 $Z \to q\bar{q}$ mode

The signal cross section of this mode is 19.8 fb. The possible background processes for this mode are $qqqq$, $qqll$, and $qql\nu$, which come from $e^+e^- \to W^+W^-$ or $e^+e^- \to ZZ$ reactions. An example diagram is shown in Figure 2-(B). Other possible backgrounds are $e^+e^- \to ZH$ with $Z \to \tau^+\tau^-$ and $H \to q\bar{q}$. These processes have the same final state to the signal.

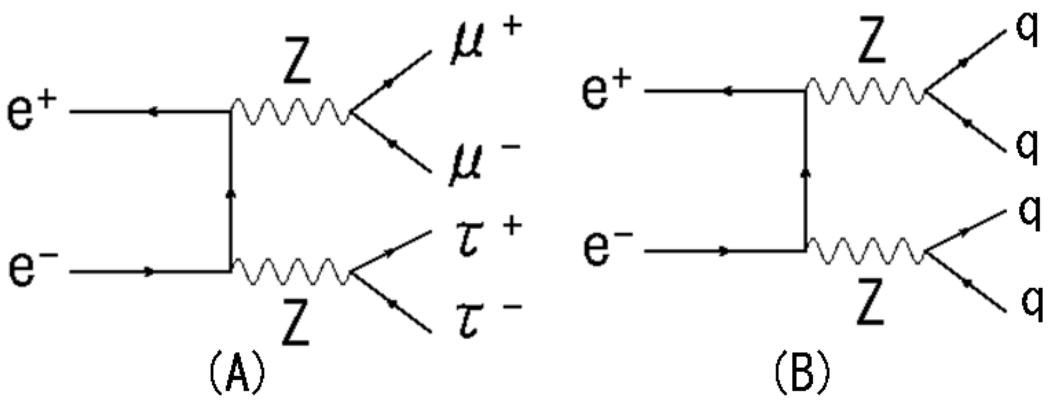

Figure 2: Example diagrams of possible background. (A): $\mu\mu\tau\tau$ background for $Z \to l^+l^-$ mode, (B): $qqqq$ background for $Z \to q\bar{q}$ mode.

3 Simulation Conditions

We performed the detector simulation with Mokka [3], a Geant4-based [4] full simulation, with the ILD_00 detector model. TAUOLA [5] was used for the tau decay simulation. The ILD_00 detector model is consists of vertex detector, time projection chamber, electromagnetic calorimeter (ECAL), hadronic calorimeter (HCAL), and yoke.

We used the signal and background samples which were generated in the context of the Letter of Intent [6]. The assumed center-of-mass energy is 250 GeV. The effects of beamstrahlung and initial state radiation are included. All Monte-Carlo sample information (process ID, process, polarization, cross section, number of events, and luminosity) are summarized in Tables 6 (page 9) and 7 (page 10). We assumed the Higgs mass $M_H = 120$ GeV, branching ratio $\mathrm{Br}(H \to \tau^+\tau^-) = 8.0$ % as assumed by PYTHIA [8], integrated luminosity $\int L\, dt = 250\ \mathrm{fb}^{-1}$, and beam polarization $P(e^+, e^-) = (+0.3, -0.8)$. We also rescale the final result to the case of $M_H = 125$ GeV and the $H \to \tau^+\tau^-$ branching ratio which includes the NNLO corrections [9].

4 Event Reconstruction and Event Selection

4.1 $Z \to l^+l^-$ mode

In this mode, we take the strategy of reconstructing the Z boson first, followed by the reconstruction of the tau pairs from the Higgs decay.

We applied lepton identification at first for dividing $Z \to e^+e^-$ events and $Z \to \mu^+\mu^-$ events by using the information of energy deposit in the calorimeter (E_{ECAL} and E_{HCAL}, where E_{ECAL} is the energy deposit in ECAL, E_{HCAL} is the energy deposit in HCAL, respectively) and track momentum (P_{track}). Figures 3 - 6 are the plots of $E_{\mathrm{ECAL}}/(E_{\mathrm{ECAL}} + E_{\mathrm{HCAL}})$ and $(E_{\mathrm{ECAL}} + E_{\mathrm{HCAL}})/P_{\mathrm{track}}$.

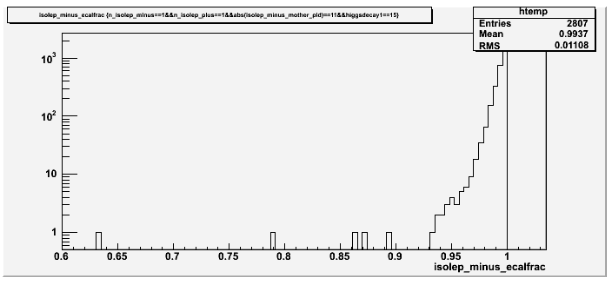

Figure 3: The plot of $E_{\mathrm{ECAL}}/(E_{\mathrm{ECAL}}+E_{\mathrm{HCAL}})$ for the e in eeH samples.

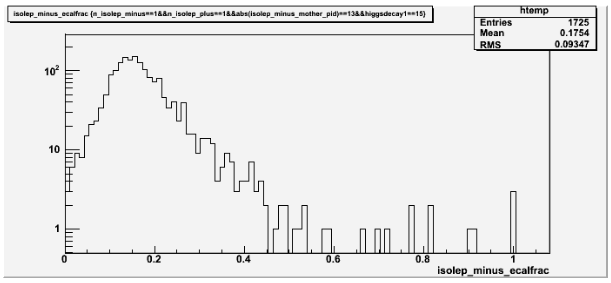

Figure 4: The plot of $E_{\mathrm{ECAL}}/(E_{\mathrm{ECAL}}+E_{\mathrm{HCAL}})$ for the μ in $\mu\mu H$ samples.

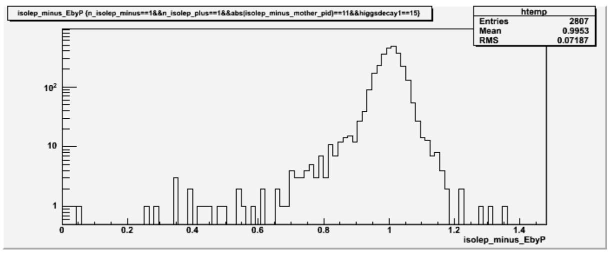

Figure 5: The plot of $(E_{\mathrm{ECAL}} + E_{\mathrm{HCAL}})/P_{\mathrm{track}}$ for the e in eeH samples.

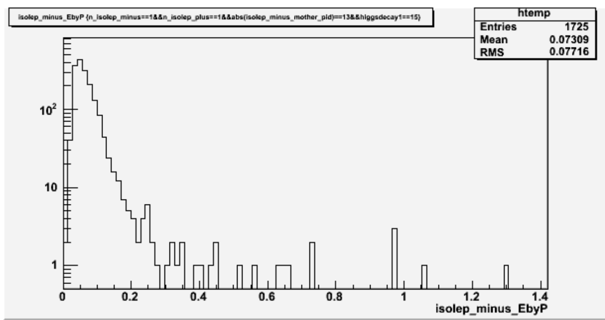

Figure 6: The plot of $(E_{\mathrm{ECAL}} + E_{\mathrm{HCAL}})/P_{\mathrm{track}}$ for the μ in $\mu\mu H$ samples.

From these plots, we define the criteria for lepton identification. The criteria for electron identification (e-ID) are: $E_{\mathrm{ECAL}}/(E_{\mathrm{ECAL}} + E_{\mathrm{HCAL}}) > 0.92$ and $(E_{\mathrm{ECAL}} + E_{\mathrm{HCAL}})/P_{\mathrm{track}} > 0.5$. The criteria for muon identification (μ-ID) are: $E_{\mathrm{ECAL}}/(E_{\mathrm{ECAL}} + E_{\mathrm{HCAL}}) < 0.6$ and $(E_{\mathrm{ECAL}} + E_{\mathrm{HCAL}})/P_{\mathrm{track}} < 0.5$.

After the lepton identification, we applied selections to remove secondary leptons from tau decays. The strategy of this selection is to remove tracks which do not come from the interaction point (IP) by using the track energy E_{track} and impact parameter in the transverse direction d_0 and longitudinal direction z_0 with respect to the beam axis. Figures 7 - 12 show the $|d_0/\sigma(d_0)|$, $|z_0/\sigma(z_0)|$, and E_{track} plots which through the lepton identification. We defined the tau rejection cut for the objects through the e-ID: $|d_0/\sigma(d_0)| < 50$, $|z_0/\sigma(z_0)| < 5$, and $E_{\mathrm{track}} > 10$ GeV, and for the objects through the μ-ID: $|d_0/\sigma(d_0)| < 3$, $|z_0/\sigma(z_0)| < 7$, and $E_{\mathrm{track}} > 20$ GeV.

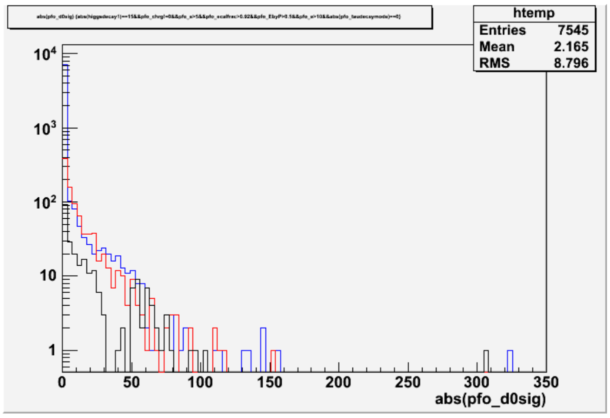

Figure 7: The plot of $|d_0/\sigma(d_0)|$ of e of eeH process. Blue, red, and black histograms show the e from $Z \to e^+e^-$, the e from $\tau \to e\nu\nu$, and the hadrons from τ decay, respectively.

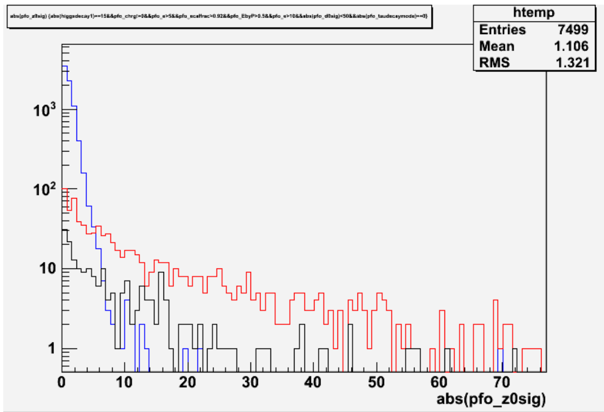

Figure 8: The plot of $|z_0/\sigma(z_0)|$ of e of eeH process. Blue, red, and black histograms show the e from $Z \to e^+e^-$, the e from $\tau \to e\nu\nu$, and the hadrons from τ decay, respectively.

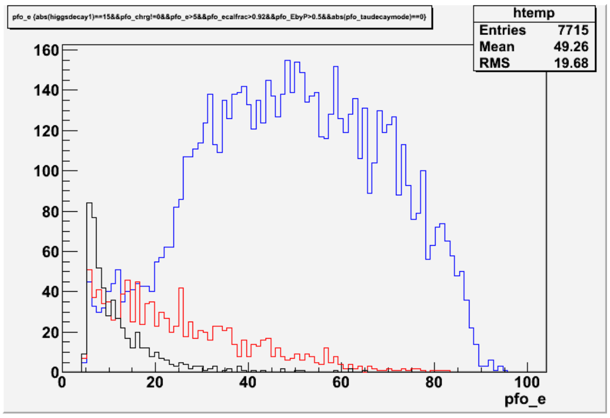

Figure 9: The plot of E_{track} of e of eeH process. Blue, red, and black histograms show the e from $Z \to e^+e^-$, the e from $\tau \to e\nu\nu$, and the hadrons from τ decay, respectively.

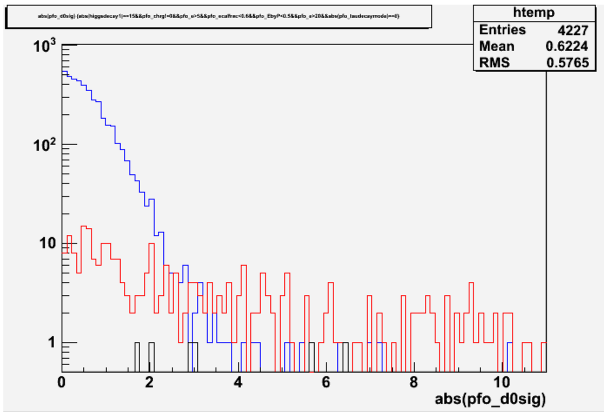

Figure 10: The plot of $|d_0/\sigma(d_0)|$ of μ of $\mu\mu H$ process. Blue, red, and black histograms show the μ from $Z \to \mu^+\mu^-$, the μ from $\tau \to \mu\nu\nu$, and the hadrons from τ decay, respectively.

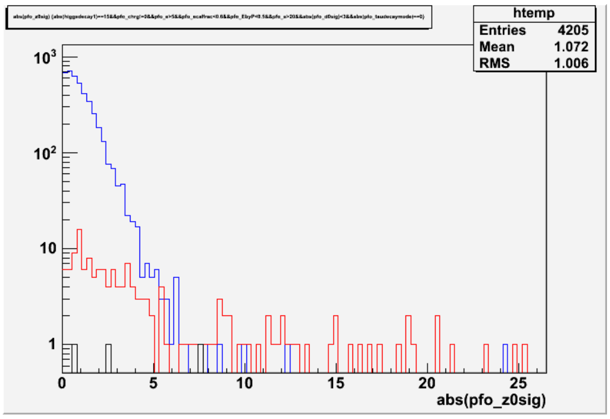

Figure 11: The plot of $|z_0/\sigma(z_0)|$ of μ of $\mu\mu H$ process. Blue, red, and black histograms show the μ from $Z \to \mu^+\mu^-$, the μ from $\tau \to \mu\nu\nu$, and the hadrons from τ decay, respectively.

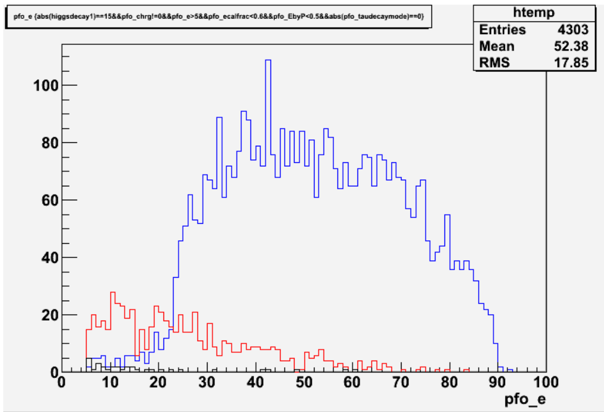

Figure 12: The plot of E_{track} of μ of $\mu\mu H$ process. Blue, red, and black histograms show the μ from $Z \to \mu^+\mu^-$, the μ from $\tau \to \mu\nu\nu$, and the hadrons from τ decay, respectively.

We applied the energy recovery procedure to correct for bremsstrahlung and final state radiation. In order to reconstruct the original Z boson, we have to use both the charged particles and the radiated photons. To achieve this, we defined the cone as shown in Figure 13. The four-momenta of the neutral particles in the cone were combined with that of the lepton candidate. We defined the half-opening angle of the cone with $\cos\theta_{\mathrm{cone}} = 0.999$ and applied the recovery procedure to the lepton candidates. The results are shown in Figures 14 and 15.

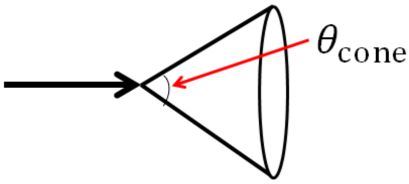

Figure 13: The definition of the cone. Black arrow shows the lepton candidate. θ_{cone} is the angle of the cone.

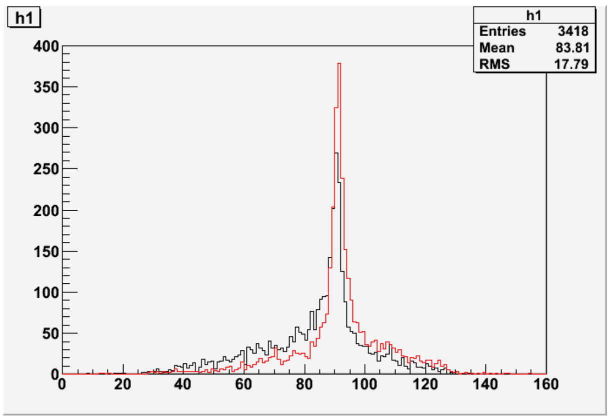

Figure 14: The results of recovery for $Z \to e^+e^-$ mode. The horizontal axis shows the M_Z. Black and red histograms show the results of without recovery and with recovery ($\cos\theta_{\mathrm{cone}} = 0.999$), respectively.

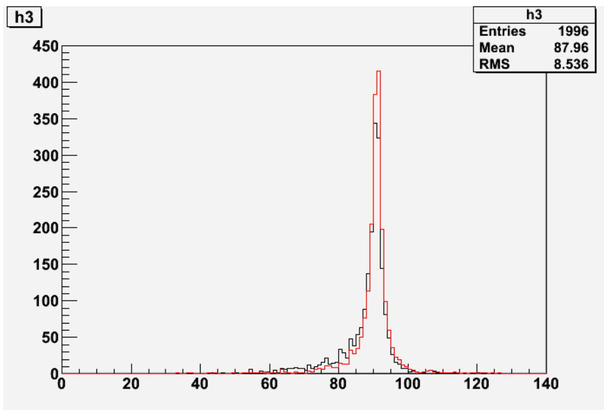

Figure 15: The results of recovery for $Z \to \mu^+\mu^-$ mode. The horizontal axis shows the M_Z. Black and red histograms show the results of without recovery and with recovery ($\cos\theta_{\mathrm{cone}} = 0.999$), respectively.

After that, we applied the tau finder to the remaining objects to reconstruct tau leptons. First of all, the objects which already used at Z boson reconstruction were rejected from tau reconstruction analysis. Then we search the highest energy track from the remaining objects, and combine the neighboring particles (which satisfies the angle with respect to the highest energy track less than 1.0 radian) with the combined mass less than 2 GeV. We regarded the combined object as a tau candidate. Then repeat these processes until there are no charged particles.

After finishing the event reconstruction, we applied the cuts for selecting signal, rejecting background. Before optimizing the cuts, we applied the preselection as follows for $Z \to e^+e^-$ mode: number of e^+ and $e^- = 1$, number of τ^+ and $\tau^- = 1$, and for $Z \to \mu^+\mu^-$ mode: number of μ^+ and $\mu^- = 1$, number of τ^+ and $\tau^- = 1$.

We applied the following cuts for $Z \to e^+e^-$ mode: number of tracks ≤ 8, 115 GeV $< E_{\text{vis}} <$ 230 GeV, $|\cos\theta_{\text{miss}}| < 0.99$, 81 GeV $< M_Z <$ 113 GeV, $\cos\theta_{e^-} < 0.92$, $\cos\theta_{e^+} > -0.92$, $E_{e^-} <$ 90 GeV, $E_{e^+} <$ 90 GeV, $\cos\theta_{\tau^+\tau^-} < -0.45$, $\cos\theta_{\tau^-} < 0.92$, $\cos\theta_{\tau^+} > -0.92$, and 116 GeV $< M_{\text{recoil}} <$ 142 GeV, where E_{vis} is the visible energy, θ_{miss} is the missing momentum angle with respect to beam axis, $\theta_{e^-(e^+)}$ is the $e^-(e^+)$ angle with respect to beam axis, $E_{e^-(e^+)}$ is the $e^-(e^+)$ energy, $\theta_{\tau^+\tau^-}$ is the angle between τ^+ and τ^-, $\theta_{\tau^-(\tau^+)}$ is the $\tau^-(\tau^+)$ angle with respect to beam axis, and M_{recoil} is the recoil mass, respectively. The histograms of all cut variables are shown in Figures 17 - 28 (page 11 - 12). Table 1 shows the cut statistics of this mode. After the cuts, the $Z \to e^+e^-$ signal events of 108.9 and background events of 76.0 remained. The statistical significance was calculated to be $S/\sqrt{S+B} = 108.9/\sqrt{108.9+76.0} = 8.0\sigma$.

We applied the following cuts for $Z \to \mu^+\mu^-$ mode: number of tracks ≤ 8, 115 GeV $< E_{\text{vis}} <$ 235 GeV, $|\cos\theta_{\text{miss}}| < 0.98$, 72 GeV $< M_Z <$ 107 GeV, $E_{e^-} <$ 90 GeV, $E_{e^+} <$ 90 GeV, $\cos\theta_{\tau^+\tau^-} < -0.5$, and 118 GeV $< M_{\text{recoil}} <$ 143 GeV. The histograms of all cut variables are shown in Figures 29 - 36 (page 13 - 14). Table 2 shows the cut statistics of this mode. For the $Z \to \mu^+\mu^-$ mode case, 131.2 signal events and 91.2 background events were remained. The significance was $S/\sqrt{S+B} = 131.2/\sqrt{131.2+91.2} = 8.8\sigma$.

Table 1: The cut statistics of $Z \to e^+e^-$ mode.

	eeH $H \to \tau\tau$	$\mu\mu H$ $H \to \tau\tau$	$\tau\tau H$ $H \to \tau\tau$	ZH with no τ	$ee\tau\tau$	other 4 leptons	other SM bkg	signi.
No cut	228.3	211.1	214.6	7325	2.388×10^5	5.238×10^5	1.492×10^{10}	0.0019
preselection	171.3	0.155	1.532	47.05	1.338×10^4	3.215×10^4	1.023×10^7	0.053
# of tracks	169.4	0.155	1.532	41.56	1.316×10^4	3.205×10^4	1.009×10^7	0.053
E_{vis}	162.3	0.155	0.912	38.36	1.068×10^4	1.039×10^4	4.761×10^6	0.074
$\cos\theta_{\text{miss}}$	160.6	0.155	0.912	38.03	8719	1906	5.155×10^5	0.22
M_Z	148.0	0	0.017	29.09	2408	501.2	1.299×10^4	1.2
$\cos\theta_{e^-(e^+)}$	133.9	0	0.009	25.40	1067	101.5	729.7	3.0
$E_{e^-(e^+)}$	133.0	0	0.009	24.93	690.3	78.70	629.7	3.4
$\cos\theta_{\tau^+\tau^-}$	130.8	0	0	3.536	254.9	30.70	155.4	5.5
$\cos\theta_{\tau^-(\tau^+)}$	123.4	0	0	3.074	212.1	9.161	3.817	6.6
M_{recoil}	108.9	0	0	2.474	72.35	1.134	0.034	8.0

Table 2: The cut statistics of $Z \to \mu^+\mu^-$ mode.

	$\mu\mu H$ $H \to \tau\tau$	eeH $H \to \tau\tau$	$\tau\tau H$ $H \to \tau\tau$	ZH with no τ	$\mu\mu\tau\tau$	other 4 leptons	other SM bkg	signi.
No cut	211.1	228.3	214.6	7325	3513	7.591×10^6	1.492×10^{10}	0.0017
preselection	168.5	0	0.155	43.01	1698	7546	7732	1.3
# of tracks	167.4	0	0.155	39.65	1684	7537	7400	1.3
E_{vis}	162.9	0	0.155	37.40	1586	2285	3713	1.9
$\cos\theta_{\text{miss}}$	158.6	0	0.155	36.51	1386	227.5	55.48	3.7
M_Z	153.2	0	0	32.84	1038	55.28	42.54	4.2
$E_{e^-(e^+)}$	153.2	0	0	32.70	738.6	42.41	36.72	4.8
$\cos\theta_{\tau^+\tau^-}$	146.3	0	0	3.638	259.4	20.19	0.756	7.1
M_{recoil}	131.2	0	0	2.875	82.36	5.311	0.301	8.8

4.2 $Z \to q\bar{q}$ mode

In this mode, the tau pairs are reconstructed first, followed by the di-jet reconstruction of the Z decay.

At first in this mode, we applied the tau finder to all objects to reconstruct tau leptons. In this analysis, we search the highest energy track and combine the neighboring particles, which satisfy $\cos\theta_{\mathrm{cone}} > 0.98$, with the combined mass less than 2 GeV. We regarded the combined object as a tau candidate. Then we applied the selection cuts as following: $E_{\mathrm{tau\ candidate}} > 3$ GeV, $E_{\mathrm{cone}} < 0.1 E_{\mathrm{tau\ candidate}}$ with $\cos\theta_{\mathrm{cone}} = 0.9$, and rejecting 3-prong with neutral particles events. These selection cuts were tuned for minimizing misidentification of part of quark jets as tau jets. The survived tau candidate regarded as a tau jet. After the selection cuts, we applied the charge recovery to obtain better efficiency. The charged particles in tau jet which have the energy less than 2 GeV are detached one by one from smallest energy from the tau jet until satisfying the conditions as following: the charge of tau jet is $+1$ or -1, and the number of track(s) in tau jet is 1 or 3. The tau jet after detaching is rejected if it does not satisfy the above conditions. After the selection cuts and detaching, we repeat the above processes until there are no charged particles which have the energy greater than 2 GeV.

After the tau reconstruction, we applied the collinear approximation [10] to reconstruct $M_{\tau^+\tau^-}$. In this approximation, we assumed that the visible decay products of tau and the neutrino(s) from tau is collinear, and the contribution of missing transverse momentum is only comes from the neutrino(s) of tau decay. The invariant mass of the tau pair with the collinear approximation shown in Figure 16.

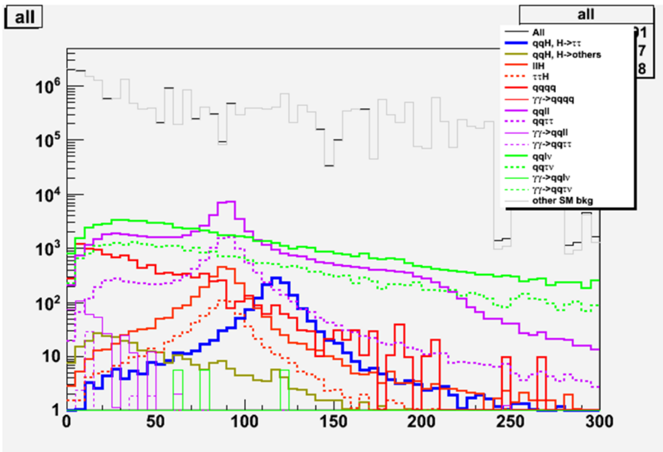

Figure 16: The plot of M_{colapp} in the unit of GeV, the invariant mass of di-tau with collinear approximation. Blue histogram shows the signal process $ZH \to qq\tau\tau$.

After that, we applied the Durham jet clustering method [11] with two jets for the remaining objects for the reconstruction of the Z boson.

After the tau and Z reconstruction, we applied the cuts to select signal process. Before optimizing cuts, we applied the preselection as follows: number of quark jets $= 2$, number of τ^+ and $\tau^- = 1$, number of tracks in $\tau \leq 3$, and the events which have the tracks in both $\tau = 3$ were rejected (double 3-prong cut). We applied the following cuts to reject the background: $9 \leq$ number of tracks < 50, 110 GeV $< E_{\mathrm{vis}} <$ 235 GeV, $|\cos\theta_{\mathrm{miss}}| < 0.98$, 77 GeV $< M_Z <$ 135 GeV, 80 GeV $< E_Z <$ 135 GeV, $\cos\theta_{\tau^+\tau^-} < -0.5$, $\log_{10}|d_0/\sigma(d_0)|(\tau^+) + \log_{10}|d_0/\sigma(d_0)|(\tau^-) > -0.7$, $\log_{10}|z_0/\sigma(z_0)|(\tau^+) + \log_{10}|z_0/\sigma(z_0)|(\tau^-) > -0.1$, $M_{\tau^+\tau^-} <$ 115 GeV, $E_{\tau^+\tau^-} <$ 125 GeV, 100 GeV $< M_{\mathrm{colapp}} <$ 170 GeV, 100 GeV $< E_{\mathrm{colapp}} <$ 280 GeV, and 112 GeV $< M_{\mathrm{recoil}} <$ 160 GeV, where $M_{\tau^+\tau^-}$ and $E_{\tau^+\tau^-}$ is the invariant mass and energy without using collinear approximation, M_{colapp} and E_{colapp} is the invariant mass and energy with collinear approximation, respectively. The histograms of all cut variables are shown in Figures 37 - 49 (page 14 - 16). Table 3 shows the cut statistics of this mode. After the cuts, the signal events and background events were remained 1026 and 554.4. The statistical significance of $Z \to q\bar{q}$ mode is calculated to be $S/\sqrt{S+B} = 1026/\sqrt{1026+554.4} = 25.8\sigma$.

Table 3: The cut statistics of $Z \to q\bar{q}$ mode.

	qqH $H \to \tau\tau$	ZH with no τ	llH	$\tau\tau H$	$qqqq$	$qqll$	$qq\tau\tau$	$ql\nu$	$qq\tau\nu$	other SM bkg	signi.
No cut	4233	4.829×10^4	5377	2596	4.038×10^6	3.563×10^5	4.169×10^4	2.788×10^6	1.326×10^6	1.494×10^{10}	0.035
preselection	1647	578.8	2761	765.4	1.230×10^4	6.378×10^4	1.161×10^4	1.249×10^5	4.948×10^4	2.570×10^7	0.32
# of tracks	1644	549.8	2680	765.4	1.230×10^4	6.059×10^4	1.146×10^4	1.214×10^5	4.806×10^4	5.190×10^5	1.9
E_{vis}	1607	492.3	1015	744.2	4443	2.106×10^4	1.107×10^4	1.192×10^5	4.693×10^4	2.383×10^5	2.4
$\cos\theta_{\text{miss}}$	1572	474.7	860.5	725.1	2127	8315	1.021×10^4	1.171×10^5	4.415×10^4	5939	3.6
M_Z	1440	376.1	791.3	682.8	778.6	4987	8674	8189	3288	997.3	8.3
E_Z	1429	352.0	782.7	528.7	505.0	4797	7857	7703	3061	609.9	8.6
$\cos\theta_{\tau^+\tau^-}$	1386	46.28	442.2	255.6	191.4	1468	2001	2831	1154	475.6	13.7
$d_0$sig	1338	30.29	235.1	244.3	131.4	854.9	1928	1786	1044	248.1	15.1
$z_0$sig	1287	19.54	105.0	234.7	81.77	408.2	1845	909.9	883.4	244.6	16.6
$M_{\tau^+\tau^-}$	1286	19.39	103.2	234.7	72.05	349.1	1837	883.5	883.4	243.9	16.7
$E_{\tau^+\tau^-}$	1282	19.39	103.0	234.7	72.05	324.7	1836	873.2	883.4	243.9	16.7
M_{colapp}	1065	3.074	18.76	47.94	10.28	72.83	616.9	150.8	137.0	0.746	23.1
E_{colapp}	1062	2.454	18.01	46.72	10.28	71.27	612.1	93.05	93.52	0.454	23.7
M_{recoil}	1026	2.144	14.54	21.24	9.938	57.07	366.3	39.64	43.31	0.161	25.8

5 Summary

We evaluated the measurement accuracy of the branching ratio of the $H \to \tau^+\tau^-$ mode at $\sqrt{s} =$ 250 GeV at the ILC with ILD_00 detector model. We assumed $M_H = 120$ GeV, $\text{Br}(H \to \tau^+\tau^-) =$ 8.0 %, $\int L\ dt = 250\ \text{fb}^{-1}$, and the polarization $P(e^+, e^-) = (+0.3, -0.8)$. The obtained values were summarized in Table 4.

Table 4: The analysis results of $\sqrt{s} = 250$ GeV.

mode	$Z \to e^+e^-$	$Z \to \mu^+\mu^-$	$Z \to q\bar{q}$
significance	8.0σ	8.8σ	25.8σ

From these results, the combined significance was calculated to be $\sqrt{8.0^2 + 8.8^2 + 25.8^2} =$ 28.4σ. Therefore, the measurement accuracy $\Delta(\sigma \cdot \text{Br})/(\sigma \cdot \text{Br})$ was calculated to be $\Delta(\sigma \cdot \text{Br})/(\sigma \cdot \text{Br}) = 1/28.4 = 3.5$ %.

The results are extrapolated to the case of $M_H = 125$ GeV by scaling the signal yields by the $e^+e^- \to ZH$ cross section and the branching ratio $\text{Br}(H \to \tau^+\tau^-) \to 6.32$ % [9]. We assumed that the selection efficiencies the same. The results are summarized in Table 5.

Table 5: The results of the extrapolation to $M_H = 125$ GeV.

$Z \to e^+e^-$	$Z \to \mu^+\mu^-$	$Z \to q\bar{q}$	Combined	$\dfrac{\Delta(\sigma \cdot \text{Br})}{\sigma \cdot \text{Br}}$
6.8σ	7.4σ	21.9σ	24.1σ	4.2 %

A Monte-Carlo Samples

Table 6: Monte-Carlo information which used in this analysis. From the left line, the process ID, process, beam polarization (ep for positrons, em for electrons), cross section in the unit of fb, number of Monte-Carlo events, integrated luminosity in the unit of fb^{-1}, are shown. This list continues to Table 7.

21564	aa_bb	ep+0.0em+0.0	960.971	96	0.099899
21565	aa_bb	ep+0.0em+0.0	5218.47	521	0.0998377
21566	aa_bb	ep+0.0em+0.0	5205.84	520	0.0998878
21567	aa_bb	ep+0.0em+0.0	4768.41	476	0.0998236
21560	aa_cc	ep+0.0em+0.0	25826.9	2582	0.0999733
21561	aa_cc	ep+0.0em+0.0	158487	15848	0.0999956
21562	aa_cc	ep+0.0em+0.0	158287	15828	0.0999956
21563	aa_cc	ep+0.0em+0.0	208135	20813	0.0999976
23532	aa_ccbb	ep+0.0em+0.0	0.010556	10	947.329
23533	aa_ccbb	ep+0.0em+0.0	0.004464	10	2240.14
23534	aa_ccbb	ep+0.0em+0.0	0.004538	10	2203.61
23432	aa_cccc	ep+0.0em+0.0	0.038923	10	256.918
23433	aa_cccc	ep+0.0em+0.0	0.012718	10	786.287
23434	aa_cccc	ep+0.0em+0.0	0.01308	10	764.526
23528	aa_ccdd	ep+0.0em+0.0	0.008955	10	1116.69
23529	aa_ccdd	ep+0.0em+0.0	0.002019	10	4952.95
23530	aa_ccdd	ep+0.0em+0.0	0.002071	10	4828.59
23516	aa_cce1e1	ep+0.0em+0.0	0.475002	10	21.0525
23517	aa_cce1e1	ep+0.0em+0.0	0.574236	10	17.4144
23518	aa_cce1e1	ep+0.0em+0.0	0.578067	10	17.299
23519	aa_cce1e1	ep+0.0em+0.0	0.095982	10	104.186
23520	aa_cce2e2	ep+0.0em+0.0	0.473937	10	21.0999
23521	aa_cce2e2	ep+0.0em+0.0	0.578748	10	17.2787
23522	aa_cce2e2	ep+0.0em+0.0	0.581645	10	17.1926
23523	aa_cce2e2	ep+0.0em+0.0	0.095404	10	104.817
23524	aa_cce3e3	ep+0.0em+0.0	0.809322	10	12.356
23525	aa_cce3e3	ep+0.0em+0.0	1.07006	10	9.34527
23526	aa_cce3e3	ep+0.0em+0.0	1.07435	10	9.30795
23527	aa_cce3e3	ep+0.0em+0.0	0.198611	10	50.3497
23392	aa_csdu	ep+0.0em+0.0	0.644164	10	15.524
23393	aa_csdu	ep+0.0em+0.0	0.001171	10	8539.71
23394	aa_csdu	ep+0.0em+0.0	0.001482	10	6747.64
23380	aa_cse1n1	ep+0.0em+0.0	0.225189	10	44.4071
23384	aa_cse2n2	ep+0.0em+0.0	0.225196	10	44.4058
23388	aa_cse3n3	ep+0.0em+0.0	0.225468	10	44.3522
23396	aa_cssc	ep+0.0em+0.0	0.650312	10	15.3772
23397	aa_cssc	ep+0.0em+0.0	0.002852	10	3506.31
23398	aa_cssc	ep+0.0em+0.0	0.003221	10	3104.63
21552	aa_dd	ep+0.0em+0.0	1611.35	161	0.0999162
21553	aa_dd	ep+0.0em+0.0	9902.35	990	0.0999763
21554	aa_dd	ep+0.0em+0.0	9913.25	991	0.0999672
21555	aa_dd	ep+0.0em+0.0	12993.6	1299	0.0999723
21536	aa_e1e1	ep+0.0em+0.0	75475.4	7547	0.0999928
21537	aa_e1e1	ep+0.0em+0.0	551033	107786	0.195607
21539	aa_e1e1	ep+0.0em+0.0	1.42431e+06	137431	0.0964895
23556	aa_e1e1bb	ep+0.0em+0.0	0.031025	10	322.321
23557	aa_e1e1bb	ep+0.0em+0.0	0.028705	10	348.371
23558	aa_e1e1bb	ep+0.0em+0.0	0.02884	10	346.741
23559	aa_e1e1bb	ep+0.0em+0.0	0.004257	10	2349.07
23549	aa_e1e1dd	ep+0.0em+0.0	0.050209	10	199.167
23550	aa_e1e1dd	ep+0.0em+0.0	0.050399	10	198.417
23551	aa_e1e1dd	ep+0.0em+0.0	0.008768	10	1140.51
23536	aa_e1e1e1e1	ep+0.0em+0.0	0.662331	10	15.0982
23537	aa_e1e1e1e1	ep+0.0em+0.0	0.971629	10	10.292
23538	aa_e1e1e1e1	ep+0.0em+0.0	0.97552	10	10.2509
23539	aa_e1e1e1e1	ep+0.0em+0.0	0.236858	10	42.2194
23540	aa_e1e1e2e2	ep+0.0em+0.0	1.68665	10	5.92891
23541	aa_e1e1e2e2	ep+0.0em+0.0	3.07145	20	6.51158
23543	aa_e1e1e2e2	ep+0.0em+0.0	0.971522	10	10.2931
23544	aa_e1e1e3e3	ep+0.0em+0.0	3.14724	10	3.17739
23545	aa_e1e1e3e3	ep+0.0em+0.0	6.49529	10	1.53958
23546	aa_e1e1e3e3	ep+0.0em+0.0	6.52147	10	1.5334
23547	aa_e1e1e3e3	ep+0.0em+0.0	2.55979	10	3.90657
23552	aa_e1e1ss	ep+0.0em+0.0	0.044906	10	222.687
23553	aa_e1e1ss	ep+0.0em+0.0	0.050028	10	199.888
23554	aa_e1e1ss	ep+0.0em+0.0	0.050343	10	198.637
23555	aa_e1e1ss	ep+0.0em+0.0	0.008754	10	1142.33
21540	aa_e2e2	ep+0.0em+0.0	75532.1	7553	0.0999972
21541	aa_e2e2	ep+0.0em+0.0	550664	55066	0.0999993
21542	aa_e2e2	ep+0.0em+0.0	551685	55168	0.0999991
21543	aa_e2e2	ep+0.0em+0.0	1.42387e+06	141987	0.0997191
23576	aa_e2e2bb	ep+0.0em+0.0	0.031069	10	321.864
23577	aa_e2e2bb	ep+0.0em+0.0	0.028705	10	348.371
23578	aa_e2e2bb	ep+0.0em+0.0	0.028893	10	346.105
23579	aa_e2e2bb	ep+0.0em+0.0	0.004264	10	2345.22
23568	aa_e2e2dd	ep+0.0em+0.0	0.044878	10	222.826
23569	aa_e2e2dd	ep+0.0em+0.0	0.050182	10	199.275
23570	aa_e2e2dd	ep+0.0em+0.0	0.050545	10	197.844
23571	aa_e2e2dd	ep+0.0em+0.0	0.008769	10	1140.38
23560	aa_e2e2e2e2	ep+0.0em+0.0	0.663421	10	15.0734
23561	aa_e2e2e2e2	ep+0.0em+0.0	0.97309	10	10.2765
23562	aa_e2e2e2e2	ep+0.0em+0.0	0.975528	10	10.2509
23563	aa_e2e2e2e2	ep+0.0em+0.0	0.236644	10	42.2576
23564	aa_e2e2e3e3	ep+0.0em+0.0	3.15328	10	3.1713
23565	aa_e2e2e3e3	ep+0.0em+0.0	6.51091	20	3.07177
23567	aa_e2e2e3e3	ep+0.0em+0.0	2.56862	10	3.89314
23572	aa_e2e2ss	ep+0.0em+0.0	0.044865	10	222.891
23573	aa_e2e2ss	ep+0.0em+0.0	0.049876	10	200.497
23574	aa_e2e2ss	ep+0.0em+0.0	0.050324	10	198.712
23575	aa_e2e2ss	ep+0.0em+0.0	0.008735	10	1144.82
21544	aa_e3e3	ep+0.0em+0.0	447301	4473	0.00999998
21545	aa_e3e3	ep+0.0em+0.0	4.00527e+06	10000	0.00249671
21546	aa_e3e3	ep+0.0em+0.0	3.99604e+06	10000	0.00250248
21547	aa_e3e3	ep+0.0em+0.0	2.06478e+07	10000	0.000484313
23592	aa_e3e3bb	ep+0.0em+0.0	0.048481	10	206.266
23593	aa_e3e3bb	ep+0.0em+0.0	0.055322	10	180.76
23594	aa_e3e3bb	ep+0.0em+0.0	0.05558	10	179.921
23595	aa_e3e3bb	ep+0.0em+0.0	0.009567	10	1045.26
23584	aa_e3e3dd	ep+0.0em+0.0	0.073276	10	136.47
23585	aa_e3e3dd	ep+0.0em+0.0	0.096953	10	103.143
23586	aa_e3e3dd	ep+0.0em+0.0	0.097375	10	102.696
23587	aa_e3e3dd	ep+0.0em+0.0	0.019565	10	511.117
23580	aa_e3e3e3e3	ep+0.0em+0.0	2.98239	10	3.35302
23581	aa_e3e3e3e3	ep+0.0em+0.0	5.81718	10	1.71905
23582	aa_e3e3e3e3	ep+0.0em+0.0	5.83263	10	1.71449
23583	aa_e3e3e3e3	ep+0.0em+0.0	2.0741	10	4.82137
23588	aa_e3e3ss	ep+0.0em+0.0	0.073357	10	136.32
23589	aa_e3e3ss	ep+0.0em+0.0	0.09712	10	102.965
23590	aa_e3e3ss	ep+0.0em+0.0	0.097381	10	102.689
23591	aa_e3e3ss	ep+0.0em+0.0	0.019638	10	509.217
23312	aa_n1e1du	ep+0.0em+0.0	0.225273	10	44.3906
23300	aa_n1e1e1n1	ep+0.0em+0.0	0.076337	10	130.998
23304	aa_n1e1e2n2	ep+0.0em+0.0	0.073443	10	136.16
23308	aa_n1e1e3n3	ep+0.0em+0.0	0.073757	10	135.58
23316	aa_n1e1sc	ep+0.0em+0.0	0.225277	10	44.3898
23436	aa_n1n1e2e2	ep+0.0em+0.0	0.003527	10	2835.27
23440	aa_n1n1e3e3	ep+0.0em+0.0	0.003793	10	2636.44
23400	aa_n1n1uu	ep+0.0em+0.0	0.002035	10	4914
23332	aa_n2e2du	ep+0.0em+0.0	0.225253	10	44.3945
23320	aa_n2e2e1n1	ep+0.0em+0.0	0.073442	10	136.162
23324	aa_n2e2e2n2	ep+0.0em+0.0	0.076285	10	131.087
23328	aa_n2e2e3n3	ep+0.0em+0.0	0.073621	10	135.831
23412	aa_n2n2cc	ep+0.0em+0.0	0.002028	10	4930.97
23456	aa_n2n2e1e1	ep+0.0em+0.0	0.003538	10	2826.46
23460	aa_n2n2e3e3	ep+0.0em+0.0	0.003797	10	2633.66
23352	aa_n3e3du	ep+0.0em+0.0	0.22566	10	44.3145
23340	aa_n3e3e1n1	ep+0.0em+0.0	0.073677	10	135.728
23344	aa_n3e3e2n2	ep+0.0em+0.0	0.073519	10	136.019
23348	aa_n3e3e3n3	ep+0.0em+0.0	0.077072	10	129.749
23356	aa_n3e3sc	ep+0.0em+0.0	0.225636	10	44.3192
23420	aa_n3n3cc	ep+0.0em+0.0	0.002032	10	4921.26
23476	aa_n3n3e1e1	ep+0.0em+0.0	0.003529	10	2833.66
23480	aa_n3n3e2e2	ep+0.0em+0.0	0.003535	10	2828.85
23416	aa_n3n3uu	ep+0.0em+0.0	0.002035	10	4914
21556	aa_ss	ep+0.0em+0.0	1612.02	161	0.0998747
21557	aa_ss	ep+0.0em+0.0	9919.95	992	0.100001
21558	aa_ss	ep+0.0em+0.0	9874.29	987	0.0999566
21559	aa_ss	ep+0.0em+0.0	13010.8	1301	0.0999939
23372	aa_uddu	ep+0.0em+0.0	0.650353	10	15.3763
23373	aa_uddu	ep+0.0em+0.0	0.002865	10	3490.4
23374	aa_uddu	ep+0.0em+0.0	0.003197	10	3127.93
23360	aa_ude1n1	ep+0.0em+0.0	0.225336	10	44.3782
23364	aa_ude2n2	ep+0.0em+0.0	0.225701	10	44.3064
23368	aa_ude3n3	ep+0.0em+0.0	0.225594	10	44.3274
23376	aa_udsc	ep+0.0em+0.0	0.643852	10	15.5315
23377	aa_udsc	ep+0.0em+0.0	0.001171	10	8539.71
23378	aa_udsc	ep+0.0em+0.0	0.001484	10	6738.54
21548	aa_uu	ep+0.0em+0.0	25709.9	2570	0.0999615
21549	aa_uu	ep+0.0em+0.0	158254	31658	0.200045
21551	aa_uu	ep+0.0em+0.0	208230	20823	0.1
23512	aa_uubb	ep+0.0em+0.0	0.010578	10	945.358
23513	aa_uubb	ep+0.0em+0.0	0.004456	10	2244.17
23514	aa_uubb	ep+0.0em+0.0	0.004531	10	2207.02
23428	aa_uucc	ep+0.0em+0.0	0.078277	10	127.751
23429	aa_uucc	ep+0.0em+0.0	0.027362	10	365.47
23430	aa_uucc	ep+0.0em+0.0	0.027931	10	358.025
23496	aa_uue1e1	ep+0.0em+0.0	0.476112	10	21.0035
23498	aa_uue1e1	ep+0.0em+0.0	0.58118	10	17.2064
23499	aa_uue1e1	ep+0.0em+0.0	0.095015	10	105.247
23500	aa_uue2e2	ep+0.0em+0.0	0.474597	10	21.0705
23502	aa_uue2e2	ep+0.0em+0.0	0.576787	10	17.3374
23503	aa_uue2e2	ep+0.0em+0.0	0.095267	10	104.968
23504	aa_uue3e3	ep+0.0em+0.0	0.808463	10	12.3691
23505	aa_uue3e3	ep+0.0em+0.0	1.07061	10	9.34047
23506	aa_uue3e3	ep+0.0em+0.0	1.07551	10	9.29791
23507	aa_uue3e3	ep+0.0em+0.0	0.19932	10	50.1706
23508	aa_uuss	ep+0.0em+0.0	0.008966	10	1115.32
23509	aa_uuss	ep+0.0em+0.0	0.001999	10	5002.5
23510	aa_uuss	ep+0.0em+0.0	0.002084	10	4798.46
23424	aa_uuuu	ep+0.0em+0.0	0.03894	10	256.805
23425	aa_uuuu	ep+0.0em+0.0	0.012785	10	782.167
23426	aa_uuuu	ep+0.0em+0.0	0.013116	10	762.428
21101	aa	ep+1.0em-1.0	49250.8	241254	4.89848
21102	aa	ep-1.0em+1.0	49267.2	237936	4.8295
21105	aaa	ep+1.0em-1.0	5300.06	26500	4.99994
21106	aaa	ep-1.0em+1.0	5298.17	26091	4.92453
21109	aaaa	ep+1.0em-1.0	324.752	1624	5.00074
21110	aaaa	ep-1.0em+1.0	323.783	1619	5.00026
21120	ae1_e1a	ep-1.0em+0.0	371863	18393	0.0494618
21121	ae1_e1a	ep-1.0em+0.0	5.36047e+06	266224	0.0496643
21122	ae1_e1a	ep+1.0em+0.0	372274	18614	0.0500008
21123	ae1_e1a	ep+1.0em+0.0	5.36372e+06	266186	0.0496271
21684	ae1_e1bb	ep-1.0em+0.0	196.883	196	0.995515
21685	ae1_e1bb	ep-1.0em+0.0	741.99	742	1.00001
21686	ae1_e1bb	ep+1.0em+0.0	235.7	235	0.99703
21687	ae1_e1bb	ep+1.0em+0.0	729.393	729	0.999461
21660	ae1_e1cc	ep-1.0em+0.0	2633.94	2633	0.999643
21661	ae1_e1cc	ep-1.0em+0.0	14122.4	14122	0.999972
21662	ae1_e1cc	ep+1.0em+0.0	2683.16	2683	0.99994
21663	ae1_e1cc	ep+1.0em+0.0	14237	14037	0.985952
21676	ae1_e1dd	ep-1.0em+0.0	262.926	262	0.996478
21677	ae1_e1dd	ep-1.0em+0.0	1209.36	1209	0.999702
21678	ae1_e1dd	ep+1.0em+0.0	305.707	305	0.997687
21679	ae1_e1dd	ep+1.0em+0.0	1204.94	1204	0.99922
21664	ae1_e1e1e1	ep-1.0em+0.0	7275.46	7275	0.999937
21665	ae1_e1e1e1	ep-1.0em+0.0	44860.5	44060	0.982156
21666	ae1_e1e1e1	ep+1.0em+0.0	7327.35	7327	0.999952
21667	ae1_e1e1e1	ep+1.0em+0.0	44910.9	44910	0.99998
21668	ae1_e1e2e2	ep-1.0em+0.0	7859.36	7859	0.999954
21669	ae1_e1e2e2	ep-1.0em+0.0	53497.7	52297	0.977556
21670	ae1_e1e2e2	ep+1.0em+0.0	7874.12	6874	0.872986
21671	ae1_e1e2e2	ep+1.0em+0.0	53695.4	52695	0.981369
21672	ae1_e1e3e3	ep-1.0em+0.0	13442.9	13442	0.999933
21673	ae1_e1e3e3	ep-1.0em+0.0	96101.5	94701	0.985427
21674	ae1_e1e3e3	ep+1.0em+0.0	13483	13283	0.985167
21675	ae1_e1e3e3	ep+1.0em+0.0	96257.6	94057	0.977138
21648	ae1_e1n2n2	ep-1.0em+0.0	33.3463	33	0.989615
21649	ae1_e1n2n2	ep-1.0em+0.0	14.4871	14	0.966377
21650	ae1_e1n2n2	ep+1.0em+0.0	52.0695	52	0.998665
21651	ae1_e1n2n2	ep+1.0em+0.0	22.6358	22	0.971912
21652	ae1_e1n3n3	ep-1.0em+0.0	33.3836	33	0.988509
21653	ae1_e1n3n3	ep-1.0em+0.0	14.5035	14	0.965284
21654	ae1_e1n3n3	ep+1.0em+0.0	52.1148	52	0.997797
21655	ae1_e1n3n3	ep+1.0em+0.0	22.6013	22	0.973395
21680	ae1_e1ss	ep-1.0em+0.0	263.497	263	0.998114
21681	ae1_e1ss	ep-1.0em+0.0	1205.28	1205	0.999768
21682	ae1_e1ss	ep+1.0em+0.0	304.802	304	0.997369
21683	ae1_e1ss	ep+1.0em+0.0	1203.83	1203	0.999311
21656	ae1_e1uu	ep-1.0em+0.0	2630.42	2630	0.99984
21657	ae1_e1uu	ep-1.0em+0.0	14117.2	14117	0.999986
21658	ae1_e1uu	ep+1.0em+0.0	2696.52	2696	0.999807
21659	ae1_e1uu	ep+1.0em+0.0	14189.1	14189	0.999993
21189	bb	ep+1.0em-1.0	47506.1	99600	2.09657
21190	bb	ep-1.0em+1.0	27566	99800	3.6204
21533	bbbb	ep+1.0em-1.0	67.0078	67008	1000
21534	bbbb	ep-1.0em+1.0	28.7721	28772	999.997
22281	bbcsdu	ep+1.0em-1.0	0.029907	10000	334370
22285	bbcssc	ep+1.0em-1.0	0.034435	10000	290402
22286	bbcssc	ep-1.0em+1.0	0.002779	10000	3.59842e+06
20633	bbh	ep+1.0em-1.0	75.602	75602	1000
20634	bbh	ep-1.0em+1.0	48.4438	48444	1000
22261	bbuddu	ep+1.0em-1.0	0.033986	10000	294239
22262	bbuddu	ep-1.0em+1.0	0.002776	10000	3.60231e+06
22265	bbudsc	ep+1.0em-1.0	0.030041	10000	332878
21165	cc	ep+1.0em-1.0	44745.7	99600	2.22591
21166	cc	ep-1.0em+1.0	27317.2	88600	3.24338
21449	ccbb	ep+1.0em-1.0	123.789	99000	799.748
21450	ccbb	ep-1.0em+1.0	56.6712	55671	982.351
21349	cccc	ep+1.0em-1.0	54.3735	53774	988.974
21350	cccc	ep-1.0em+1.0	26.3297	26330	1000.01
24477	ccccbb	ep+1.0em-1.0	0.003422	10000	2.92227e+06
24478	ccccbb	ep-1.0em+1.0	0.001756	10000	5.69476e+06
21445	ccdd	ep+1.0em-1.0	120.779	100000	827.959
21446	ccdd	ep-1.0em+1.0	55.1663	54566	989.118
24773	ccddbb	ep+1.0em-1.0	0.004519	10000	2.21288e+06
24774	ccddbb	ep-1.0em+1.0	0.002267	10000	4.41112e+06
21432	cce1e1	ep-1.0em-1.0	448.721	96400	214.833
21433	cce1e1	ep+1.0em-1.0	506.805	98000	193.368
21434	cce1e1	ep-1.0em+1.0	464.383	96800	208.449
21435	cce1e1	ep+1.0em+1.0	448.339	99200	221.261
21437	cce2e2	ep+1.0em-1.0	53.1354	52935	996.229
21438	cce2e2	ep-1.0em+1.0	29.3345	29335	1000.02
21441	cce3e3	ep+1.0em-1.0	52.7484	52548	996.201
21442	cce3e3	ep-1.0em+1.0	29.1511	29151	999.997
20609	cch	ep+1.0em-1.0	59.231	59231	1000
20610	cch	ep-1.0em+1.0	37.8798	37880	1000.01
21309	csdu	ep+1.0em-1.0	6513.67	99600	15.2909
21310	csdu	ep-1.0em+1.0	59.9344	59534	993.319
21297	cse1n1	ep+1.0em-1.0	2466.05	92400	37.4688
21298	cse1n1	ep-1.0em+1.0	20.9278	11528	550.846
21299	cse1n1	ep+1.0em+1.0	86.2613	80061	928.122
21301	cse2n2	ep+1.0em-1.0	2268.39	100000	44.0841
21302	cse2n2	ep-1.0em+1.0	20.8866	20887	1000.02
21305	cse3n3	ep+1.0em-1.0	2266.29	100000	44.125
21306	cse3n3	ep-1.0em+1.0	20.8669	20867	1000
21313	cssc	ep+1.0em-1.0	6638.5	99800	15.0335
21314	cssc	ep-1.0em+1.0	112.648	79200	703.075
21181	dd	ep+1.0em-1.0	48065.6	100000	2.08049
21182	dd	ep-1.0em+1.0	28036.9	99200	3.53819
21521	ddbb	ep+1.0em-1.0	137.124	90200	657.799
21522	ddbb	ep-1.0em+1.0	58.9095	58909	999.992
21513	dddd	ep+1.0em-1.0	67.066	66666	994.036
21514	dddd	ep-1.0em+1.0	28.8606	24661	854.487
24973	ddddbb	ep+1.0em-1.0	0.001092	10000	9.15751e+06
20625	ddh	ep+1.0em-1.0	75.8898	75890	1000
20626	ddh	ep-1.0em+1.0	48.5522	48552	999.996
21517	ddss	ep+1.0em-1.0	134.545	65800	489.056
21518	ddss	ep-1.0em+1.0	57.7479	51748	896.102
24981	ddssbb	ep+1.0em-1.0	0.002197	10000	4.55166e+06
24982	ddssbb	ep-1.0em+1.0	0.001108	10000	9.02527e+06
21116	e1a_e1a	ep+0.0em-1.0	372192	18610	0.0500011
21117	e1a_e1a	ep+0.0em-1.0	5.39497e+06	269148	0.0498887
21118	e1a_e1a	ep+0.0em+1.0	372426	18621	0.0499992
21119	e1a_e1a	ep+0.0em+1.0	5.39207e+06	267003	0.0495177
21624	e1a_e1bb	ep+0.0em-1.0	235.778	235	0.9967
21625	e1a_e1bb	ep+0.0em-1.0	729.568	729	0.999221
21626	e1a_e1bb	ep+0.0em+1.0	196.862	196	0.995621
21627	e1a_e1bb	ep+0.0em+1.0	742.713	742	0.99904

Table 7: Monte-Carlo information which used in this analysis. From the left line, the process ID, process, beam polarization (ep for positrons, em for electrons), cross section in the unit of fb, number of Monte-Carlo events, integrated luminosity in the unit of fb^{-1}, are shown. This list is series of Table 6.

21600	e1a_e1cc	ep+0.0em-1.0	2692.03	2000	0.742934
21601	e1a_e1cc	ep+0.0em-1.0	14238.4	14238	0.999972
21602	e1a_e1cc	ep+0.0em+1.0	2630.76	2630	0.999711
21603	e1a_e1cc	ep+0.0em+1.0	14172	14172	1
21616	e1a_e1dd	ep+0.0em-1.0	305.228	305	0.999253
21617	e1a_e1dd	ep+0.0em-1.0	1207.73	1207	0.999396
21618	e1a_e1dd	ep+0.0em+1.0	263.602	263	0.997716
21619	e1a_e1dd	ep+0.0em+1.0	1210.08	1210	0.999934
21604	e1a_e1e1e1	ep+0.0em-1.0	7311.26	7311	0.999964
21605	e1a_e1e1e1	ep+0.0em-1.0	45047.7	43047	0.955587
21606	e1a_e1e1e1	ep+0.0em+1.0	7282.56	7282	0.999923
21607	e1a_e1e1e1	ep+0.0em+1.0	44999.4	43999	0.977769
21608	e1a_e1e2e2	ep+0.0em-1.0	7880.39	7880	0.99995
21609	e1a_e1e2e2	ep+0.0em-1.0	53812.4	53412	0.992559
21610	e1a_e1e2e2	ep+0.0em+1.0	7869.66	7869	0.999916
21611	e1a_e1e2e2	ep+0.0em+1.0	53765.8	50565	0.940468
21612	e1a_e1e3e3	ep+0.0em-1.0	13471.9	13471	0.999933
21613	e1a_e1e3e3	ep+0.0em-1.0	96603.4	94803	0.981363
21614	e1a_e1e3e3	ep+0.0em+1.0	13459.7	13459	0.999948
21615	e1a_e1e3e3	ep+0.0em+1.0	96607	95607	0.989649
21588	e1a_e1n2n2	ep+0.0em-1.0	52.0727	52	0.998604
21589	e1a_e1n2n2	ep+0.0em-1.0	21.8282	21	0.962058
21590	e1a_e1n2n2	ep+0.0em+1.0	33.307	33	0.990783
21591	e1a_e1n2n2	ep+0.0em+1.0	13.982	14	1.00129
21592	e1a_e1n3n3	ep+0.0em-1.0	52.0479	52	0.99908
21593	e1a_e1n3n3	ep+0.0em-1.0	21.8319	21	0.961895
21594	e1a_e1n3n3	ep+0.0em+1.0	33.3573	33	0.989289
21595	e1a_e1n3n3	ep+0.0em+1.0	13.9806	14	1.00139
21620	e1a_e1ss	ep+0.0em-1.0	305.28	305	0.999083
21621	e1a_e1ss	ep+0.0em-1.0	1203.61	1203	0.999493
21622	e1a_e1ss	ep+0.0em+1.0	263.322	263	0.998777
21623	e1a_e1ss	ep+0.0em+1.0	1210.02	1210	0.999983
21596	e1a_e1uu	ep+0.0em-1.0	2697.07	2697	0.999974
21597	e1a_e1uu	ep+0.0em-1.0	14270.7	14270	0.999951
21598	e1a_e1uu	ep+0.0em+1.0	2631.22	2631	0.999916
21599	e1a_e1uu	ep+0.0em+1.0	14186.3	14186	0.999979
21168	e1e1	ep-1.0em-1.0	1.72542e+07	25000	0.00144892
21169	e1e1	ep+1.0em-1.0	1.73374e+07	22500	0.00129777
21170	e1e1	ep-1.0em+1.0	1.72946e+07	24500	0.00141663
21171	e1e1	ep+1.0em+1.0	1.72517e+07	25000	0.00144913
21472	e1e1bb	ep-1.0em-1.0	57.2207	57221	1000.01
21473	e1e1bb	ep+1.0em-1.0	106.063	100000	942.836
21474	e1e1bb	ep-1.0em+1.0	68.9777	68978	1000
21475	e1e1bb	ep+1.0em+1.0	57.3099	57310	1000
21464	e1e1dd	ep-1.0em-1.0	73.3921	72592	989.098
21465	e1e1dd	ep+1.0em-1.0	123.983	100000	806.562
21466	e1e1dd	ep-1.0em+1.0	85.3261	84126	985.935
21467	e1e1dd	ep+1.0em+1.0	73.442	73442	1000
21452	e1e1e1e1	ep-1.0em-1.0	942.464	92200	97.8287
21453	e1e1e1e1	ep+1.0em-1.0	995.595	91400	91.8044
21454	e1e1e1e1	ep-1.0em+1.0	982.404	97400	99.1445
21455	e1e1e1e1	ep+1.0em+1.0	943.694	97800	103.635
21456	e1e1e2e2	ep-1.0em-1.0	1073.64	100000	93.1411
21457	e1e1e2e2	ep+1.0em-1.0	1106.71	99800	90.1772
21458	e1e1e2e2	ep-1.0em+1.0	1088.6	100000	91.8611
21459	e1e1e2e2	ep+1.0em+1.0	1068.97	99000	92.6125
21460	e1e1e3e3	ep-1.0em-1.0	941.685	98800	104.918
21461	e1e1e3e3	ep+1.0em-1.0	965.145	97800	101.332
21462	e1e1e3e3	ep-1.0em+1.0	948.774	99000	104.345
21463	e1e1e3e3	ep+1.0em+1.0	942.984	98200	104.138
20612	e1e1h	ep-1.0em-1.0	0.644995	10000	15504
20613	e1e1h	ep+1.0em-1.0	17.8919	17892	1000.01
20614	e1e1h	ep-1.0em+1.0	11.2894	11289	999.965
20615	e1e1h	ep+1.0em+1.0	0.645477	10000	15492.4
21468	e1e1ss	ep-1.0em-1.0	73.2531	73253	999.999
21469	e1e1ss	ep+1.0em-1.0	123.972	100000	806.634
21470	e1e1ss	ep-1.0em+1.0	85.4529	65600	767.674
21471	e1e1ss	ep+1.0em+1.0	73.152	71752	980.862
21173	e2e2	ep+1.0em-1.0	17077.6	99000	5.79707
21174	e2e2	ep-1.0em+1.0	12859.5	99400	7.72969
21493	e2e2bb	ep+1.0em-1.0	56.5071	56307	996.459
21494	e2e2bb	ep-1.0em+1.0	29.5793	28779	972.944
21485	e2e2dd	ep+1.0em-1.0	57.5377	57538	1000.01
21486	e2e2dd	ep-1.0em+1.0	30.2016	30202	1000.01
21477	e2e2e2e2	ep+1.0em-1.0	11.4311	11431	999.991
21478	e2e2e2e2	ep-1.0em+1.0	7.23464	10000	1382.24
21481	e2e2e3e3	ep+1.0em-1.0	23.1405	23140	999.978
21482	e2e2e3e3	ep-1.0em+1.0	14.6585	14658	999.966
20617	e2e2h	ep+1.0em-1.0	17.126	17126	1000
20618	e2e2h	ep-1.0em+1.0	10.9671	10967	999.991
21489	e2e2ss	ep+1.0em-1.0	57.6073	57607	999.995
21490	e2e2ss	ep-1.0em+1.0	30.1803	29980	993.363
21177	e3e3	ep+1.0em-1.0	17102.4	98800	5.77697
21178	e3e3	ep-1.0em+1.0	12852.9	99800	7.76478
21509	e3e3bb	ep+1.0em-1.0	56.1355	55535	989.303
21510	e3e3bb	ep-1.0em+1.0	29.4194	29219	993.188
21501	e3e3dd	ep+1.0em-1.0	57.2295	56830	993.019
21502	e3e3dd	ep-1.0em+1.0	30.0379	29838	993.345
21497	e3e3e3e3	ep+1.0em-1.0	11.4274	11427	999.965
21498	e3e3e3e3	ep-1.0em+1.0	7.21497	9800	1358.29
20621	e3e3h	ep+1.0em-1.0	17.0988	17099	1000.01
20622	e3e3h	ep-1.0em+1.0	10.9435	10944	1000.05
21505	e3e3ss	ep+1.0em-1.0	57.3548	57155	996.516
21506	e3e3ss	ep-1.0em+1.0	30.0502	30050	999.993
21228	n1e1du	ep-1.0em-1.0	86.3492	86349	999.998
21229	n1e1du	ep+1.0em-1.0	2467.16	100000	40.5324
21230	n1e1du	ep-1.0em+1.0	20.8701	20870	999.995
21216	n1e1e1n1	ep-1.0em-1.0	43.5841	43384	995.409
21217	n1e1e1n1	ep+1.0em-1.0	939.099	98800	105.207
21218	n1e1e1n1	ep-1.0em+1.0	27.4575	26858	978.166
21219	n1e1e1n1	ep+1.0em+1.0	43.6248	43625	1000
21220	n1e1e2n2	ep-1.0em-1.0	28.824	28424	986.123
21221	n1e1e2n2	ep+1.0em-1.0	822.5	98000	119.149
21222	n1e1e2n2	ep-1.0em+1.0	7.09688	10000	1409.07
21224	n1e1e3n3	ep-1.0em-1.0	28.6769	28477	993.029
21225	n1e1e3n3	ep+1.0em-1.0	823.729	97800	118.728
21226	n1e1e3n3	ep-1.0em+1.0	7.10283	10000	1407.89
21232	n1e1sc	ep-1.0em-1.0	86.1229	86123	1000
21233	n1e1sc	ep+1.0em-1.0	2470.34	100000	40.4803
21234	n1e1sc	ep-1.0em+1.0	20.9005	20701	990.455
21125	n1n1a	ep+1.0em-1.0	23969.4	238694	9.95828
21126	n1n1a	ep-1.0em+1.0	2878.85	27788	9.65247
21137	n1n1aa	ep+1.0em-1.0	1582.94	15829	9.99975
21138	n1n1aa	ep-1.0em+1.0	281.145	2811	9.9984
21149	n1n1aaa	ep+1.0em-1.0	69.1909	692	10.0013
21150	n1n1aaa	ep-1.0em+1.0	16.0647	161	10.022
21369	n1n1bb	ep+1.0em-1.0	85.7148	85715	1000
21370	n1n1bb	ep-1.0em+1.0	25.0179	25018	1000
21321	n1n1cc	ep+1.0em-1.0	81.3195	81319	999.994
21322	n1n1cc	ep-1.0em+1.0	24.5259	24526	1000
21361	n1n1dd	ep+1.0em-1.0	87.9093	87909	999.997
21362	n1n1dd	ep-1.0em+1.0	25.5486	25549	1000.02
21353	n1n1e2e2	ep+1.0em-1.0	44.7068	42707	955.269
21354	n1n1e2e2	ep-1.0em+1.0	12.8466	12847	1000.03
21357	n1n1e3e3	ep+1.0em-1.0	44.4167	43417	977.493
21358	n1n1e3e3	ep-1.0em+1.0	12.7892	12789	999.984
20593	n1n1h	ep+1.0em-1.0	60.8309	60831	1000
20594	n1n1h	ep-1.0em+1.0	21.6813	21681	999.986
21365	n1n1ss	ep+1.0em-1.0	87.6368	87637	1000
21366	n1n1ss	ep-1.0em+1.0	25.4646	25465	1000.02
21317	n1n1uu	ep+1.0em-1.0	81.2845	81084	997.533
21318	n1n1uu	ep-1.0em+1.0	24.5303	24330	991.835
21249	n2e2du	ep+1.0em-1.0	2268.24	98600	43.4698
21250	n2e2du	ep-1.0em+1.0	20.8833	19883	952.1
21237	n2e2e1n1	ep+1.0em-1.0	822.267	95800	116.507
21238	n2e2e1n1	ep-1.0em+1.0	7.11354	10000	1405.77
21239	n2e2e1n1	ep+1.0em+1.0	28.8352	28835	999.993
21241	n2e2e2n2	ep+1.0em-1.0	779.633	98800	126.726
21242	n2e2e2n2	ep-1.0em+1.0	19.3972	18197	938.125
21245	n2e2e3n3	ep+1.0em-1.0	755.228	97400	128.968
21246	n2e2e3n3	ep-1.0em+1.0	7.11024	9400	1322.04
21253	n2e2sc	ep+1.0em-1.0	2265.78	97000	42.8109
21254	n2e2sc	ep-1.0em+1.0	20.8933	20493	980.841
21129	n2n2a	ep+1.0em-1.0	4486.97	42870	9.55433
21130	n2n2a	ep-1.0em+1.0	2875.61	28756	9.99996
21141	n2n2aa	ep+1.0em-1.0	439.022	4390	9.9995
21142	n2n2aa	ep-1.0em+1.0	280.164	2802	10.0013
21153	n2n2aaa	ep+1.0em-1.0	25.1552	252	10.0178
21154	n2n2aaa	ep-1.0em+1.0	16.0995	161	10.0003
21389	n2n2bb	ep+1.0em-1.0	59.3921	47792	804.686
21390	n2n2bb	ep-1.0em+1.0	24.9283	24928	999.988
21329	n2n2cc	ep+1.0em-1.0	54.498	54498	1000
21330	n2n2cc	ep-1.0em+1.0	24.5273	24327	991.834
21381	n2n2dd	ep+1.0em-1.0	60.6737	60474	996.709
21382	n2n2dd	ep-1.0em+1.0	25.509	25509	1000
21372	n2n2e1e1	ep-1.0em-1.0	16.1179	15718	975.189
21373	n2n2e1e1	ep+1.0em-1.0	38.3067	37307	973.903
21374	n2n2e1e1	ep-1.0em+1.0	21.4025	21403	1000.02
21375	n2n2e1e1	ep+1.0em+1.0	16.124	16124	1000
21377	n2n2e3e3	ep+1.0em-1.0	24.5789	24579	1000
21378	n2n2e3e3	ep-1.0em+1.0	12.7721	11772	921.697
20597	n2n2h	ep+1.0em-1.0	33.8385	33839	1000.01
20598	n2n2h	ep-1.0em+1.0	21.6474	21647	999.982
21385	n2n2ss	ep+1.0em-1.0	60.5318	56932	940.53
21386	n2n2ss	ep-1.0em+1.0	25.5038	24304	952.956
21325	n2n2uu	ep+1.0em-1.0	54.5125	52513	963.32
21326	n2n2uu	ep-1.0em+1.0	24.5195	24519	999.98
21269	n3e3du	ep+1.0em-1.0	2264.41	99000	43.72
21270	n3e3du	ep-1.0em+1.0	20.8481	20248	971.216
21257	n3e3e1n1	ep+1.0em-1.0	821.691	98000	119.266
21258	n3e3e1n1	ep-1.0em+1.0	7.10352	9600	1351.44
21259	n3e3e1n1	ep+1.0em+1.0	28.6767	28677	1000.01
21261	n3e3e2n2	ep+1.0em-1.0	755.344	99800	132.125
21262	n3e3e2n2	ep-1.0em+1.0	7.10407	10000	1407.64
21265	n3e3e3n3	ep+1.0em-1.0	777.523	99800	128.356
21266	n3e3e3n3	ep-1.0em+1.0	19.3359	19136	989.662
21273	n3e3sc	ep+1.0em-1.0	2267.88	97600	43.0358
21274	n3e3sc	ep-1.0em+1.0	20.906	20906	1000
21133	n3n3a	ep+1.0em-1.0	4488.88	44889	10
21134	n3n3a	ep-1.0em+1.0	2885	28850	10
21145	n3n3aa	ep+1.0em-1.0	440.452	4405	10.0011
21146	n3n3aa	ep-1.0em+1.0	280.722	2807	9.99922
21157	n3n3aaa	ep+1.0em-1.0	25.0412	250	9.98355
21158	n3n3aaa	ep-1.0em+1.0	16.0991	161	10.0006
21409	n3n3bb	ep+1.0em-1.0	59.3812	59381	999.997
21410	n3n3bb	ep-1.0em+1.0	24.936	24936	1000
21337	n3n3cc	ep+1.0em-1.0	54.5355	54335	996.323
21338	n3n3cc	ep-1.0em+1.0	24.532	24132	983.695
21401	n3n3dd	ep+1.0em-1.0	60.5857	60586	1000
21402	n3n3dd	ep-1.0em+1.0	25.5446	25545	1000.02
21392	n3n3e1e1	ep-1.0em-1.0	16.1083	16108	999.981
21393	n3n3e1e1	ep+1.0em-1.0	38.2851	37732	985.553
21394	n3n3e1e1	ep-1.0em+1.0	21.4031	20403	953.273
21395	n3n3e1e1	ep+1.0em+1.0	16.1459	16146	1000.01
21397	n3n3e2e2	ep+1.0em-1.0	24.7238	24324	983.829
21398	n3n3e2e2	ep-1.0em+1.0	12.8475	12847	999.961
20601	n3n3h	ep+1.0em-1.0	33.8138	33814	1000.01
20602	n3n3h	ep-1.0em+1.0	21.6936	21694	1000.02
21405	n3n3ss	ep+1.0em-1.0	60.567	60567	1000
21406	n3n3ss	ep-1.0em+1.0	25.5558	25556	1000.01
21333	n3n3uu	ep+1.0em-1.0	54.5087	54109	992.667
21334	n3n3uu	ep-1.0em+1.0	24.5484	24348	991.836
21185	ss	ep+1.0em-1.0	48249.2	98200	2.03527
21186	ss	ep-1.0em+1.0	28018.8	99400	3.54762
21529	ssbb	ep+1.0em-1.0	137.055	100000	729.634
21530	ssbb	ep-1.0em+1.0	58.9474	58947	999.993
20629	ssh	ep+1.0em-1.0	75.8803	75880	999.996
20630	ssh	ep-1.0em+1.0	48.5657	48566	1000.01
21525	ssss	ep+1.0em-1.0	67.1388	66739	994.045
21526	ssss	ep-1.0em+1.0	28.8318	28832	1000.01
24993	ssssbb	ep+1.0em-1.0	0.001091	10000	9.1659e+06
21289	uddu	ep+1.0em-1.0	6633.45	100000	15.0751
21290	uddu	ep-1.0em+1.0	112.876	99400	880.612
21277	ude1n1	ep+1.0em-1.0	2467.75	98200	39.7933
21278	ude1n1	ep-1.0em+1.0	20.8973	20897	999.986
21279	ude1n1	ep+1.0em+1.0	86.4364	86036	995.368
21281	ude2n2	ep+1.0em-1.0	2268.37	89800	39.5879
21282	ude2n2	ep-1.0em+1.0	20.9171	19717	942.626
21285	ude3n3	ep+1.0em-1.0	2263.51	100000	44.1792
21286	ude3n3	ep-1.0em+1.0	20.8931	20893	999.995
21293	udsc	ep+1.0em-1.0	6522.1	98600	15.1178
21294	udsc	ep-1.0em+1.0	59.9897	59190	986.669
21161	uu	ep+1.0em-1.0	44890.2	89800	2.00044
21162	uu	ep-1.0em+1.0	27372	95400	3.48531
21429	uubb	ep+1.0em-1.0	123.961	99400	801.865
21430	uubb	ep-1.0em+1.0	56.7304	56330	992.942
21345	uucc	ep+1.0em-1.0	109.296	99200	907.627
21346	uucc	ep-1.0em+1.0	52.8917	52892	1000.01
24457	uuccbb	ep+1.0em-1.0	0.006837	10000	1.46263e+06
24458	uuccbb	ep-1.0em+1.0	0.003574	10000	2.79799e+06
21412	uue1e1	ep-1.0em-1.0	448.519	99800	222.51
21413	uue1e1	ep+1.0em-1.0	505.705	100000	197.744
21414	uue1e1	ep-1.0em+1.0	464.733	100000	215.177
21415	uue1e1	ep+1.0em+1.0	449.636	99200	220.623
21417	uue2e2	ep+1.0em-1.0	53.0187	53019	1000.01
21418	uue2e2	ep-1.0em+1.0	29.2736	29274	1000.01
21421	uue3e3	ep+1.0em-1.0	52.7824	52582	996.203
21422	uue3e3	ep-1.0em+1.0	29.0929	27893	958.756
20605	uuh	ep+1.0em-1.0	59.1744	59174	999.993
20606	uuh	ep-1.0em+1.0	37.9259	37926	1000
21425	uuss	ep+1.0em-1.0	120.989	98800	816.603
21426	uuss	ep-1.0em+1.0	55.1501	53950	978.239
24713	uussbb	ep+1.0em-1.0	0.004512	10000	2.21631e+06
24714	uussbb	ep-1.0em+1.0	0.002273	10000	4.39947e+06
21341	uuuu	ep+1.0em-1.0	54.3813	50981	937.473
21342	uuuu	ep-1.0em+1.0	26.3337	26134	992.417
24441	uuuubb	ep+1.0em-1.0	0.003435	10000	2.91121e+06
24442	uuuubb	ep-1.0em+1.0	0.001759	10000	5.68505e+06

B Histograms of cut variables

B.1 $Z \to e^+e^-$ mode

Figures 17 - 28 show the histograms of cut variables. The blue lines in all histograms show the signal process $ZH \to e^+e^-\tau^+\tau^-$.

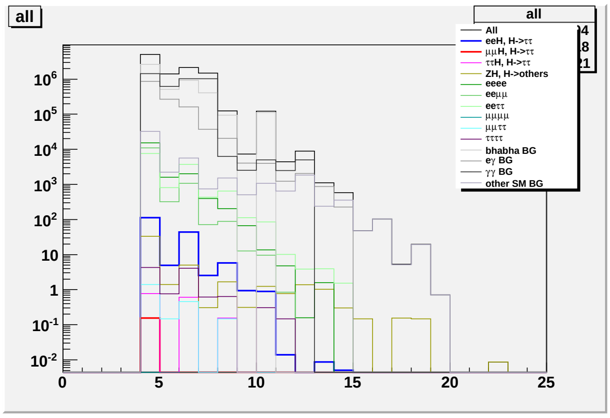

Figure 17: Number of tracks ≤ 8.

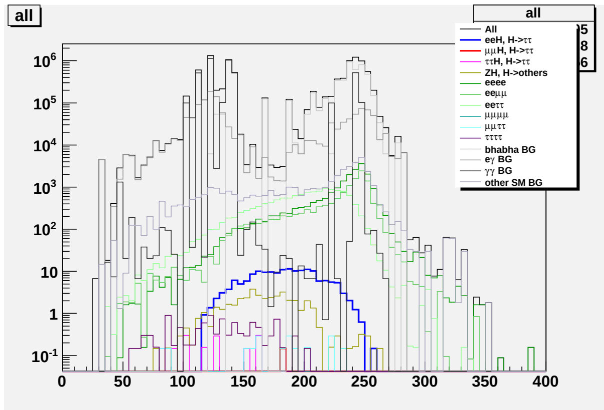

Figure 18: 115 GeV $< E_{\text{vis}} <$ 230 GeV.

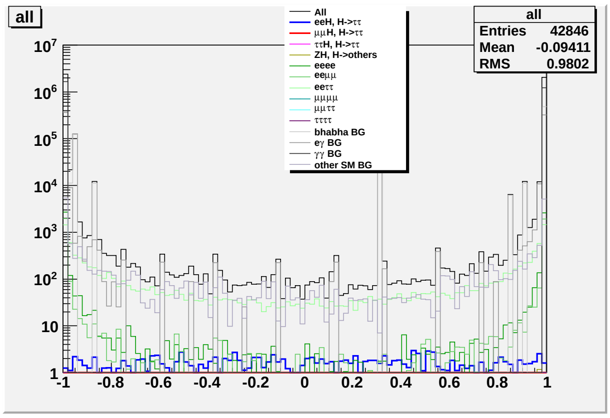

Figure 19: $|\cos\theta_{\text{miss}}| < 0.99$.

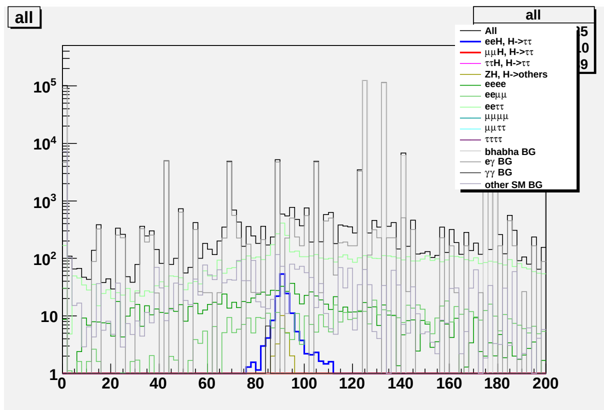

Figure 20: 81 GeV $< M_Z <$ 113 GeV.

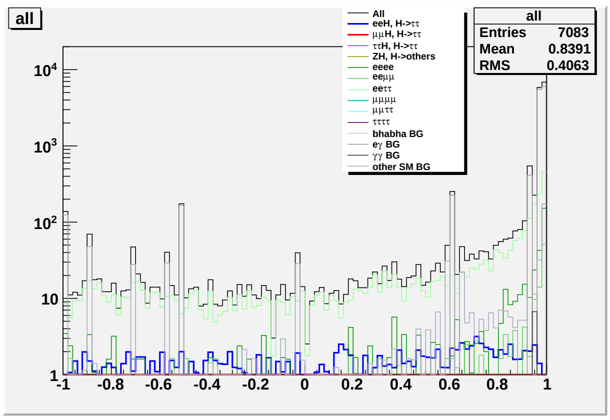

Figure 21: $\cos\theta_{e^-} < 0.92$.

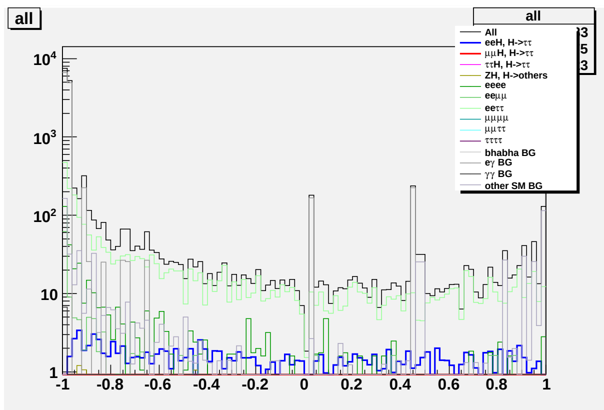

Figure 22: $\cos\theta_{e^+} > -0.92$.

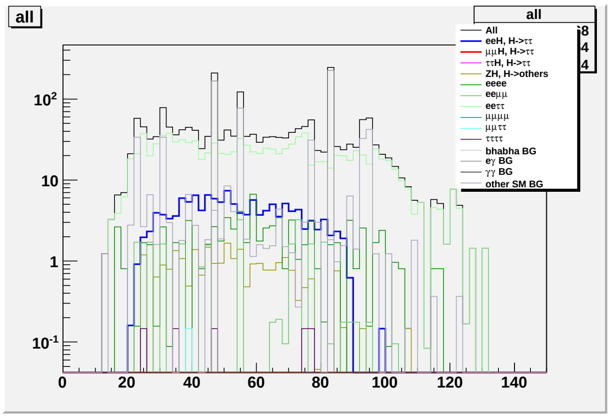

Figure 23: $E_{e^-} < 90$ GeV.

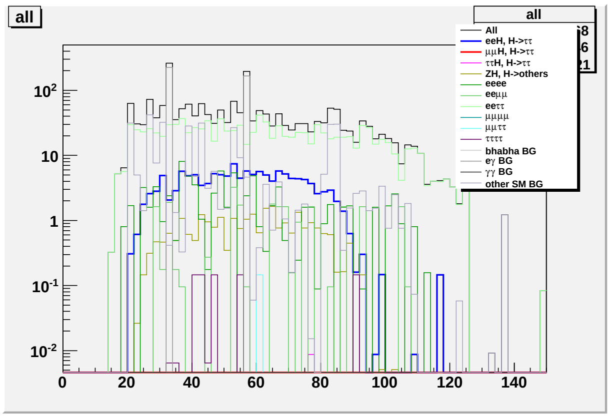

Figure 24: $E_{e^+} < 90$ GeV.

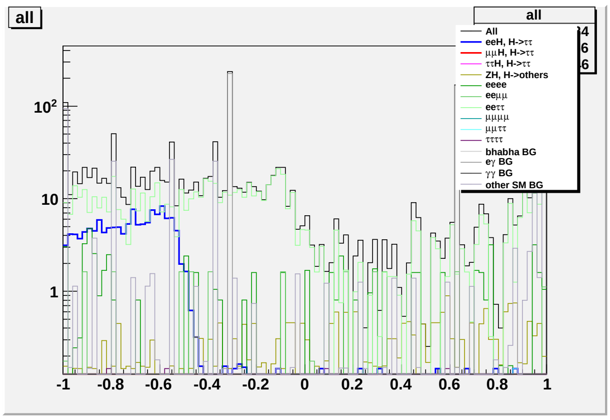

Figure 25: $\cos\theta_{\tau^+\tau^-} < -0.45$.

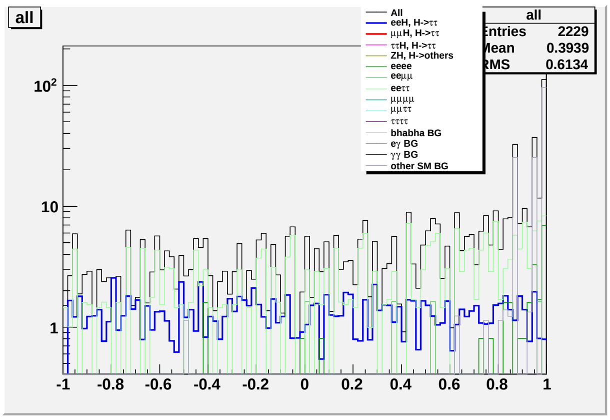

Figure 26: $\cos\theta_{\tau^-} < 0.92$.

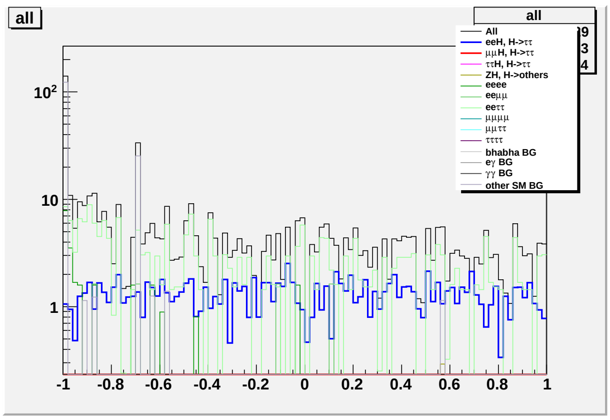

Figure 27: $\cos\theta_{\tau^+} > -0.92$.

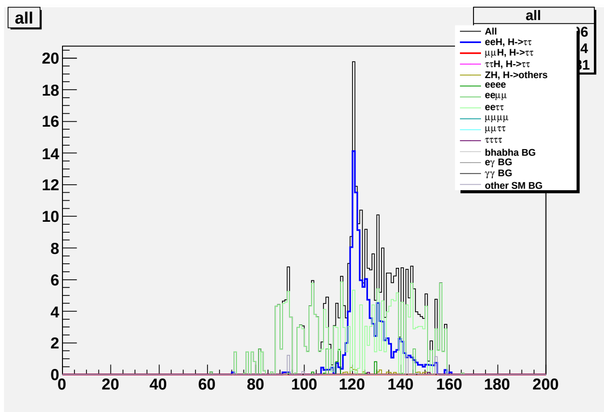

Figure 28: 116 GeV $< M_{\rm recoil} <$ 142 GeV.

B.2 $Z \to \mu^+\mu^-$ mode

Figures 29 - 36 show the histograms of cut variables. The red lines in all histograms show the signal process $ZH \to \mu^+\mu^-\tau^+\tau^-$.

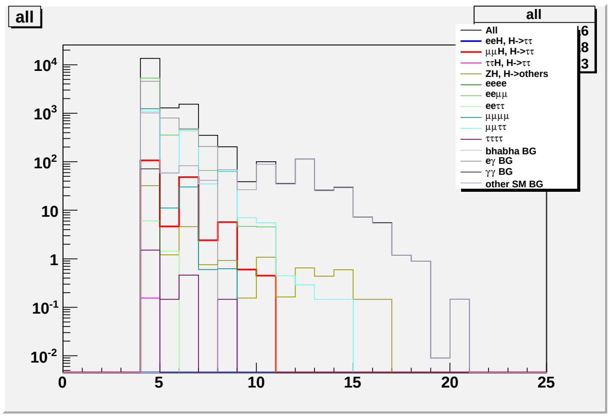

Figure 29: Number of tracks ≤ 8.

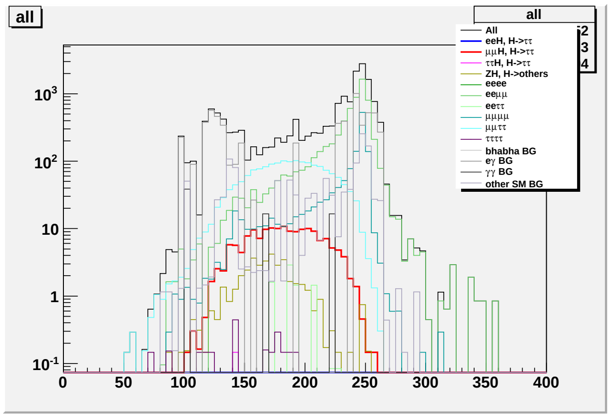

Figure 30: 115 GeV $< E_{\rm vis} <$ 235 GeV.

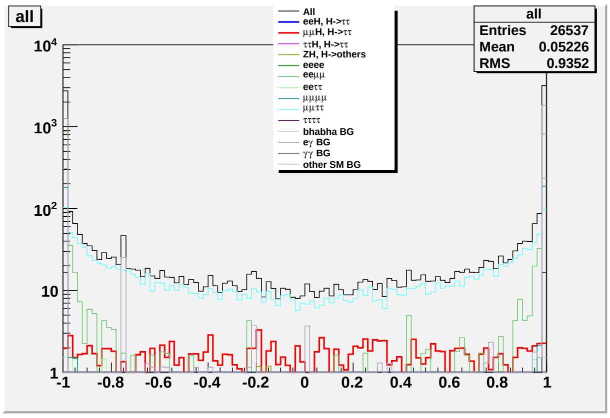

Figure 31: $|\cos\theta_{\rm miss}| < 0.98$.

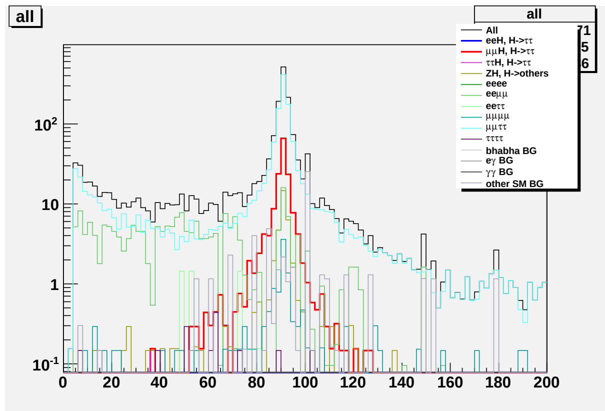

Figure 32: 72 GeV $< M_Z <$ 107 GeV.

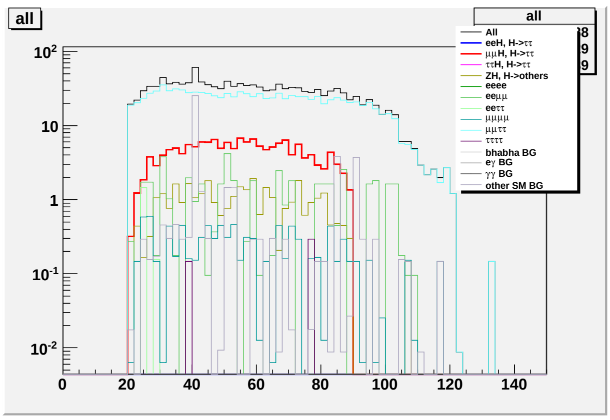

Figure 33: $E_{e^-} <$ 90 GeV.

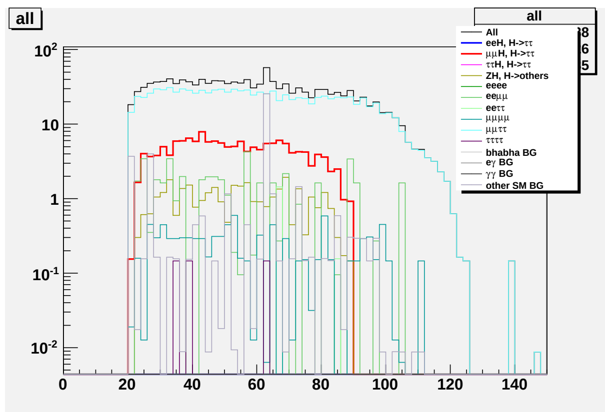

Figure 34: $E_{e^+} <$ 90 GeV.

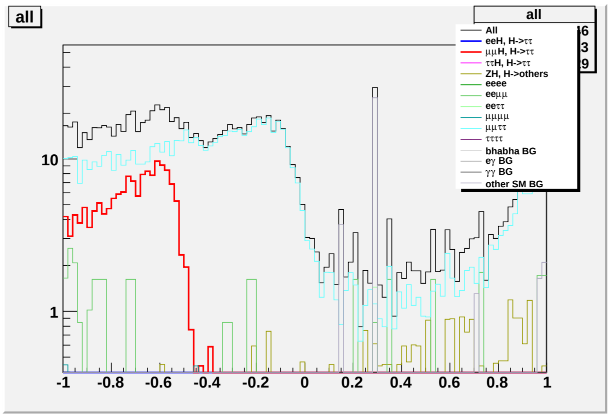

Figure 35: $\cos\theta_{\tau^+\tau^-} < -0.5$.

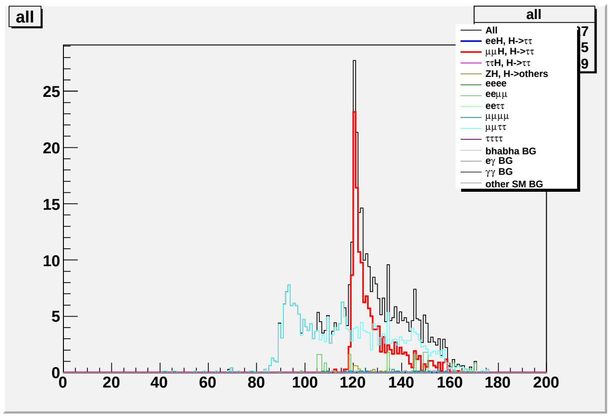

Figure 36: 118 GeV $< M_{\mathrm{recoil}} <$ 143 GeV.

B.3 $Z \to q\bar{q}$ mode

Figures 37 - 49 show the histograms of cut variables. The blue lines in all histograms show the signal process $ZH \to q\bar{q}\tau^+\tau^-$.

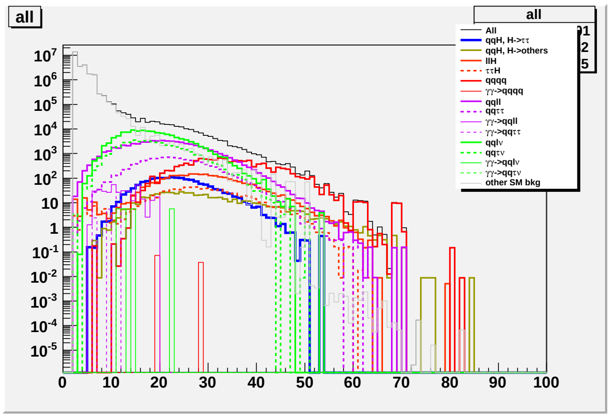

Figure 37: $9 \leq$ number of tracks < 50.

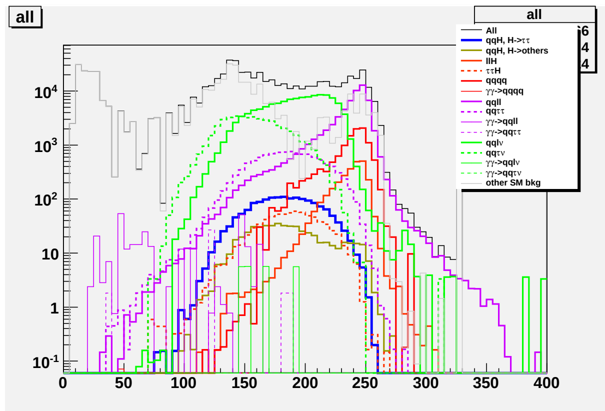

Figure 38: 110 GeV $< E_{\mathrm{vis}} <$ 235 GeV.

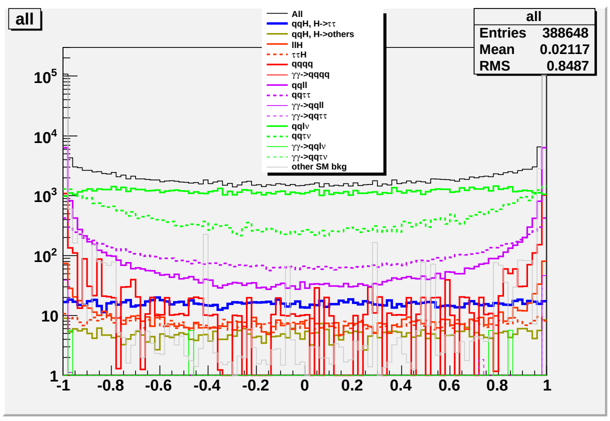

Figure 39: $|\cos\theta_{\mathrm{miss}}| < 0.98$.

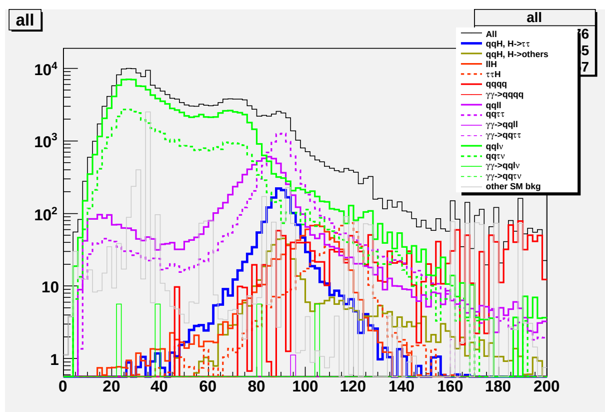

Figure 40: 77 GeV $< M_Z <$ 135 GeV.

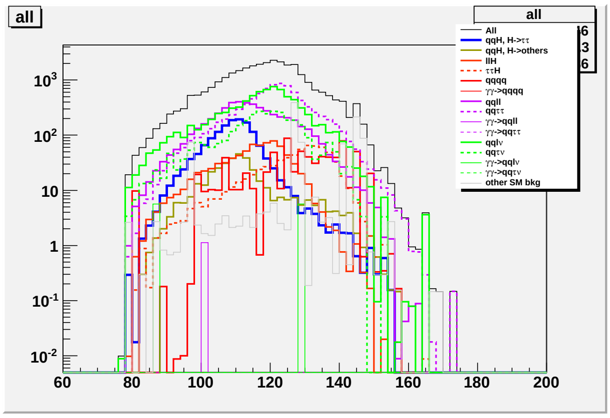

Figure 41: 80 GeV $< E_Z <$ 135 GeV.

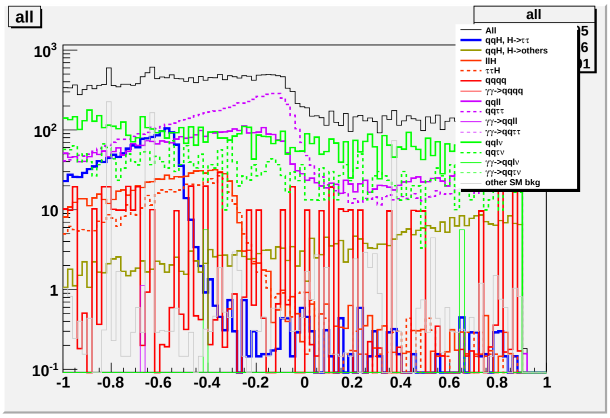

Figure 42: $\cos\theta_{\tau^+\tau^-} < -0.5$.

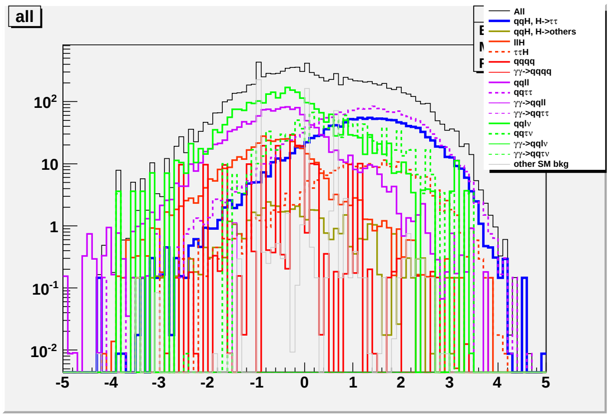

Figure 43: $\log_{10}(|d_0/\sigma(d_0)|)(\tau^-) + \log_{10}(|d_0/\sigma(d_0)|)(\tau^+) > -0.7$.

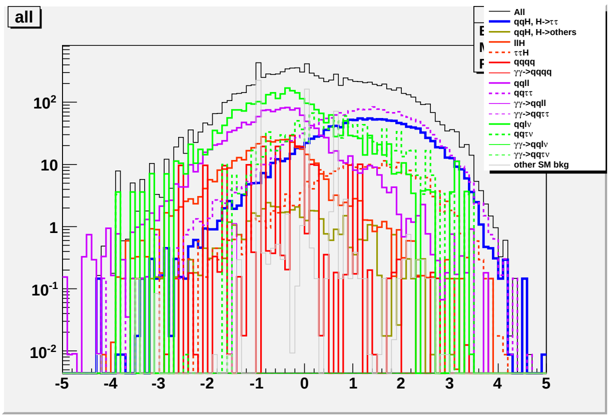

Figure 44: $\log_{10}(|z_0/\sigma(z_0)|)(\tau^-) + \log_{10}(|z_0/\sigma(z_0)|)(\tau^+) > -0.1$.

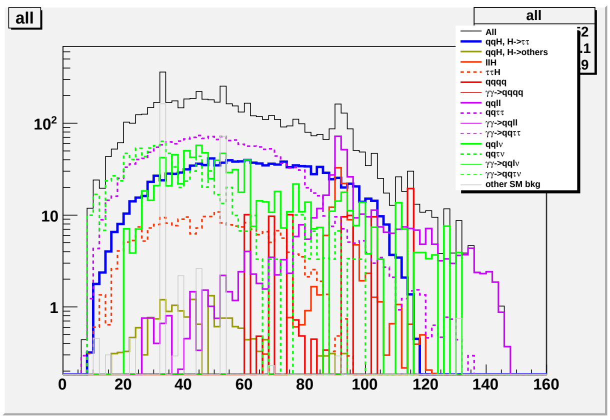

Figure 45: $M_{\tau^+\tau^-} <$ 115 GeV.

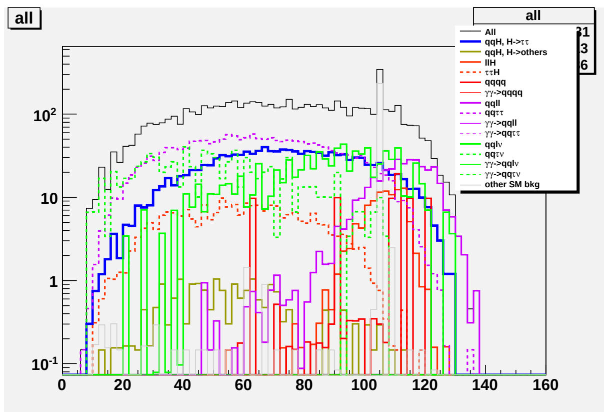

Figure 46: $E_{\tau^+\tau^-} <$ 125 GeV.

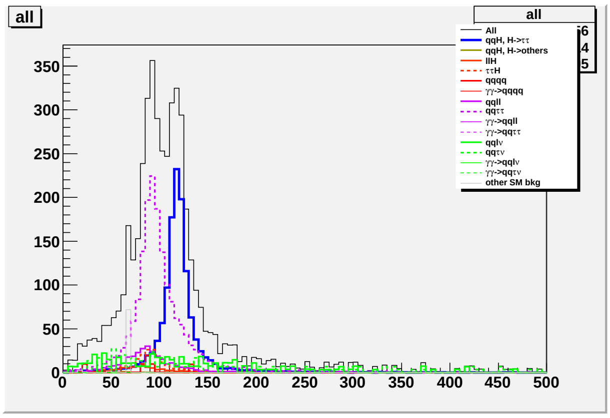

Figure 47: 100 GeV $< M_{\mathrm{colapp}} <$ 170 GeV.

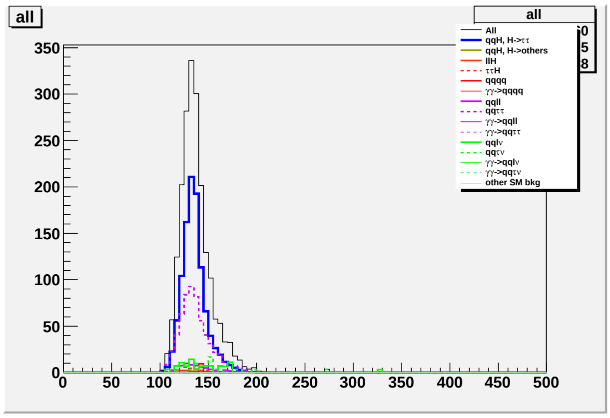

Figure 48: 100 GeV $< E_{\mathrm{colapp}} <$ 280 GeV.

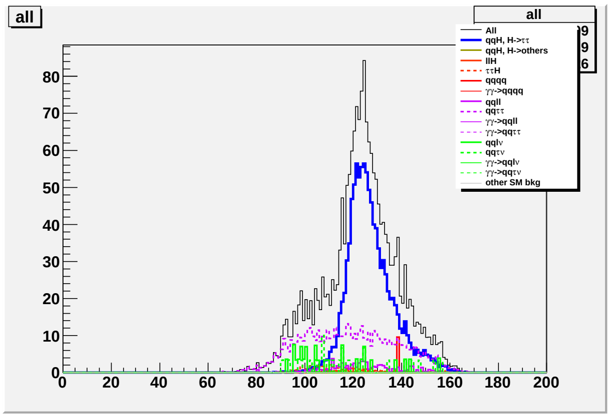

Figure 49: 112 GeV $< M_{\mathrm{recoil}} <$ 160 GeV.

References

[1] The ATLAS Collaboration, "Observation of a new particle in the search for the Standard Model Higgs boson with the ATLAS detector at the LHC", Physics Letters B **716** (2012) 1 - 29

[2] The CMS Collaboration, "Observation of a new boson at a mass of 125 GeV with the CMS experiment at the LHC", Physics Letters B **716** (2012) 30 - 61

[3] P. Mora de Fretias, H. Videau, "Detector simulation with Mokka/Geant4 present and future", LC-TOOL-2003-010 (2003)

[4] `http://geant4.cern.ch/`

[5] S. Jadach, J. H. Kühn, Z. Was, "TAUOLA — a library of Monte Carlo programs to simulate decays of polarized τ leptons", Computer Physics Communications **64** (1991) 275 - 299

[6] The ILD concept group, "International Large Detector — Letter of Intent" (2010)

[7] `http://ilcsoft.desy.de/portal`

[8] T. Sjöstrand, S. Mrenna, P. Skands, "PYTHIA 6.4 physics and manual", Journal of High Energy Phyiscs 0605, 026 (2006)

[9] LHC Higgs Cross Section Working Group, "Handbook of LHC Higgs Cross Sections: 2. Differential Distributions", arXiv:1201.3084v1 [hep-ph]

[10] R. K. Ellis, I. Hinchliffe, M. Soldate, J. J. van der bij, "Higgs decay to $\tau^+\tau^-$ A possible signature of intermediate mass Higgs bosons at high energy hadron colliders", Nuclear Physics B **297** (1988) 221 - 243

[11] S. Catani, Y. L. Dokshitzer, M. Olsson, G. Turnock, B. R. Webber, "New clustering algorithm for multijet cross sections in e^+e^- annihilation", Physics Letters B **269** (1991) 432 - 438